Leaf wax *n*-alkane variation in *Dodonaea viscosa* along an environmental gradient

Thesis submitted in accordance with the requirements of the University of Adelaide for an Honours Degree in Geology

Ellyse Bunney

November 2015

THE UNIVERSITY of ADELAIDE

LEAF WAX *N*-ALKANE VARIATION IN *DODONAEA VISCOSA* ALONG AN ENVIRONMENTAL GRADIENT

N-ALKANE VARIATION WITHIN SPECIES

ABSTRACT

The variation in distribution and abundance of leaf wax *n*-alkanes has been proposed as a proxy for palaeoclimate. Understanding environmental controls on the variation in distribution and abundance of leaf wax *n*-alkanes is therefore necessary to determine if this is a robust tool for extracting climatic information from palaeo archives. Results of previous work to create a modern baseline for this proxy have, in some cases, been confounded by differences in species or plant type between sites or along gradients. This study investigates leaf wax *n*-alkane variation within a species of Australian shrub, *Dodonaea viscosa,* which inhabits a wide range of climatic conditions.

Leaf wax *n*-alkane data from 43 individuals of *D.viscosa* were analysed from a climatic gradient ranging from central Australia to Kangaroo Island, with a mean annual temperature range of 13.9—22.7 °C and precipitation range of 164—808 mm/yr. Concentration of *n*-alkanes increase with increasing temperature along the gradient. Annual mean aridity index has the strongest relationship with the average chain length (ACL) of leaf wax *n*-alkanes and suggests that water availability is a strong driver of variation in ACL. In addition to *n*-alkane data, carbon isotope ratio ($\delta^{13}C$) and specific leaf area (SLA) data were measured to determine if this species shows predictable responses to these established and climatically sensitive leaf traits. Predicted responses in $\delta^{13}C$ and SLA are observed in this species. Only weak effects of subspecies on leaf trait relationships with climate are found in this study. Scanning electron microscopy

was used to qualitatively assess differences in leaf wax microstructure with climate and produced inconclusive results.

Distributions of leaf wax *n*-alkanes have great potential as a proxy for palaeoclimate. Results presented here support the use of *n*-alkane ACL variation to detect aridity rather than temperature.

KEYWORDS

Palaeoecology, palaeoclimate proxy, *n*-alkane, leaf wax, carbon isotopes ratios, climate, specific leaf area, Australia, *Dodonaea viscosa*.

TABLE OF CONTENTS

LIST OF FIGURES

LIST OF TABLES

INTRODUCTION

Understanding past climate change on different time scales is crucial to our ability to plan for future climate change (Bradley 2015). Instrumental records of environmental parameters do not go back far enough to be able to study the full range of climate variability (Bradley 2015). To overcome this, it is possible to use a variety of proxies that preserve information about the environment both from modern and ancient ecosystems that can be used in the absence of direct measurements (Diefendorf et al. 2011, Bradley 2015)

One potential proxy for past climates, gains information from changes in the composition of leaf waxes (Eglinton and Hamilton 1967, Eglinton and Eglinton 2008). Leaf waxes are a part of the cuticle of the leaf and provide a barrier to protect the plant from non-stomatal water loss, solar radiation and pathogens while also repelling external water (Koch and Ensikat 2008). Leaf waxes contain *n*-alkanes, which are straight, long chain hydrocarbons that have commonly been used as a fossil vegetation biomarker (Eglinton and Eglinton 2008). Fossil biomarkers are robust molecules that can be extracted from sediments and are specific to a particular biological source (Eglinton and Eglinton 2008). Research into *n*-alkane biomarkers initially focused on their potential as chemotaxonomic indicators, using the variation in *n*- alkanes to distinguish between different plant types. Bush and McInerney (2013) found that with the exception of differentiating sphagnum moss from woody angiosperms, *n*-alkane biomarkers were not a reliable tool for chemotaxonomy. However, *n*-alkane biomarkers may be sensitive to climatic variables and these could provide a potential palaeoclimate

proxy (Bush and McInerney 2013, Bush and McInerney 2015). To understand and interpret these proxy signals in fossil or sedimentary records in order to detect environmental change, it is necessary to first understand what drives *n*-alkane variation in the leaf waxes of modern plants.

Studies have shown that the melting point and hydrophobicity of *n*-alkanes increases with chain length (Eglinton and Eglinton 2008, Koch and Ensikat 2008). Longer *n*-alkanes are therefore likely to increase the effectiveness of the cuticle as a barrier to non-stomatal water loss and increase resistance of leaf waxes to heat degradation. These properties are likely to be advantageous in hot and/or dry environments, however the synthesis of longer chain lengths may have an energetic cost leading to a potential fitness trade-off between their advantageous properties and their cost of production (Riederer and Schneider 1990). The distribution of *n*-alkane chain lengths present in leaf wax may also affect the permeability of the wax layer (Riederer and Schneider 1990, Dodd and Afzal-Rafii 2000). Less variable, narrowly distributed chain lengths produce a wax layer that is more crystalline and less permeable (Riederer and Schneider 1990, Dodd and Afzal-Rafii 2000).

***Hypothesis 1*:** In hot or dry climates plants produce narrowly distributed, long chained *n*-alkanes.

Leaf wax *n*-alkanes are well suited for use as proxies to detect past environmental change as the long, straight chained compounds are chemically stable, insoluble in water and have low volatility which makes them able to persist in the environment for hundreds of millions of years (Eglinton and Eglinton 2008, Whiteside et al. 2010).

These biomarkers are continuously deposited in the environment through leaf fall or as aerosols due to wind abrasion or vegetation fires (Eglinton and Eglinton 2008). *n*-Alkane biomarkers are also source specific (Eglinton and Eglinton 2008). Terrestrial plants show a characteristic *n*-alkane profile with compounds generally ranging between 21 and 39 carbons long with one or two dominant chain lengths (Eglinton and Eglinton 2008). These profiles also show a strong odd over even chain length preference due to n-alkanes being synthesised by the removal of one carbon from alkanoic acids, which have even numbered carbon chain lengths (Eglinton and Eglinton 2008).

Leaf wax *n*-alkanes can be characterized in a number of ways. The distribution of chain length can be measured as weighted average chain length (ACL) (Carr et al. 2014).

$$ACL_{25-35} = \frac{25C_{25}+27C_{27}+29C_{29}+31C_{31}+33C_{33}+35C_{35}}{C_{25}+C_{27}+C_{29}+C_{31}+C_{33}+C_{35}} \quad (1)$$

where C_x is the concentration of the *n*-alkane (*C*) with *x* carbons.

Dispersion (d) measures the variation of chain lengths around the average chain length (Dodd et al. 1998, Dodd and Afzal-Rafii 2000).

$$d = \sum \%C_n(n - ACL)^2 \quad (2)$$

where n is the number of carbons (C_{21}–C_{35}).

Norm31 is another parameter that has been identified as being sensitive to climate and uses the proportion of C_{31} relative to C_{29} (Carr et al. 2014).

$$Norm31 = C_{31}/(C_{31} + C_{29}) \quad (3)$$

where C_x is the concentration of the *n*-alkane (*C*) with *x* carbons.

Abundance or concentration of n-alkanes can be characterised as mass of *n*-alkanes per dry leaf weight or mass of *n*-alkanes per leaf area (Eglinton and Eglinton 2008).

Attempts to correlate leaf wax composition with climatic parameters have yielded variable results. Some studies identified mean annual temperature (MAT) as the main driver of ACL variation with summer temperature having an even stronger correlation with ACL (Diefendorf et al. 2011, Tipple and Pagani 2013, Bush and McInerney 2015). In these studies average chain length increased with increasing temperatures. Other studies found aridity or water availability to be the main driver of ACL variation, with ACL increasing with increasing aridity (Hoffmann et al. 2013, Carr et al. 2014). Interestingly, in the same study Hoffmann et al. (2013) observed the opposite trend in *Acacia* where ACL decreased with increasing aridity. Dodd and Afzal-Rafii (2000) found high ACL and low dispersion corresponded with warm/dry environments and lower ACL and higher dispersion corresponded with cool/wet environments.

In addition to changes in leaf wax composition, environmental conditions may influence surface architecture of leaf waxes. Changes in wax crystal morphology of surface leaf waxes with climate have previously been investigated qualitatively using scanning electron microscopy (Koch et al. 2006). The micromorphology of wax crystals in *Brassica* has been documented to change with changes in relative humidity (Koch et al. 2006).

***Hypothesis 2*:** Crystal morphology of surface leaf waxes will change over a climatic gradient.

Variation in leaf wax composition could represent a biochemical response to climatic stress (Bush and McInerney 2015). To test this, leaf wax *n*-alkanes can be measured across a climatic gradient to determine if significant relationships exist between the two.

However, to validate the assumption that the plant of interest is experiencing stress due to climate conditions over such a gradient, other well established plant traits are available that indicate plant responses to environmental stress (Farquhar et al. 1989, Schulze et al. 2006). Changes in foliar carbon isotope ratio ($\delta^{13}C_{leaf}$) result from a physiological response to water stress (Farquhar et al. 1989, Diefendorf et al. 2010, Ma et al. 2012, Wang et al. 2013). Plant anatomical responses that are commonly measured to assess plant stress due to climate conditions include changes in leaf width, area, thickness and a range of other morphological traits (Schulze et al. 2006). Measurements of these leaf traits can be thought of as indications of the climate experienced by the plant. These established metrics will be used to test whether or not plants in this study show the predicted responses to environmental stress.

The ratio of light to heavy carbon isotopes ($\delta^{13}C$) in plants has been identified as relating to two main components. The first is the internal concentration of CO_2 inside the leaf (c_i) compared to ambient concentration of CO_2 (c_a) which can be affected by factors such as stomatal conductance and photosynthetic rate (Farquhar et al. 1989, Xiao et al. 2013). The second is the fractionation of CO_2 relative to the atmosphere that occurs during photosynthesis (O'Leary 1988, Farquhar et al. 1989). $\delta^{13}C$ is calculated as:

$$\delta^{13}C_{leaf} = \delta^{13}C_{atm} - a - (b-a)\, c_i/c_a \qquad (4)$$

where a is the fractionation factor associated with diffusion through the air and b is the fractionation factor associated with carboxylation during photosynthesis (Xiao et al. 2013).

Environmental factors influence c_i:c_a including aridity and light availability. In arid environments, plants decrease stomatal conductance by closing stomata to reduce water loss, this decreases the supply of CO_2 to the interior of the leaf (O'Leary 1988, Farquhar et al. 1989). High light availability can increase photosynthetic rate, which increases consumption of CO_2 within the leaf (O'Leary 1988). Aforementioned environmental factors (e.g. aridity) will produce a decrease in c_i compared to c_a. Low c_i:c_a results in less negative values of $\delta^{13}C$.

Trends seen in studies of $\delta^{13}C$ of C_3 plants along environmental gradients have found that less negative values correspond with more arid environments and also with increased water use efficiency in plants (Farquhar et al. 1989, Diefendorf et al. 2010, Prentice et al. 2011, Ma et al. 2012, Wang et al. 2013).

***Hypothesis 3*:** $\delta^{13}C$ values in leaves become less negative with increasing aridity.

Leaves that are smaller and thicker have a lower surface area compared to large and thin leaves. Leaves with a smaller surface area are less susceptible to desiccation, so it is likely that hot and dry climates will select for smaller and thicker leaves to limit water loss (Schulze et al. 2006). Specific Leaf Area (SLA) is defined as leaf area/leaf dry mass (cm^2/g) (Schulze et al. 2006). Small and thick leaves have a lower SLA compared to large, thin leaves. A low SLA has been associated with hot and arid environments (Schulze et al. 2006).

Hypothesis 4: Leaf SLA values decrease with increasing aridity.

This study aims to investigate the factors that influence the abundance and distribution of leaf wax *n*-alkanes. This will be achieved by measuring the composition of leaf waxes along a contemporary climate gradient. To reduce variation in the dataset, *n*-alkanes will be measured in *Dodonaea viscosa,* a single species with a wide habitat range. *D.viscosa* has seven subspecies, two of which occur along the climatic gradient in this study. With a dataset of *n*-alkane, $\delta^{13}C$ and SLA measurements from 43 individuals this study aims to:

1. Quantify variation in the abundance and distribution of leaf wax *n*-alkanes along a climate gradient and look for correlations between these traits and environmental parameters.
2. Qualitatively assess leaf wax morphology along a climate gradient.
3. Quantify the variation of stable carbon isotopes and SLA to verify that *D.viscosa* is experiencing climatic stress over this gradient and to examine correlations between these climatically sensitive parameters and the abundance and distribution of *n*-alkanes.
4. Compare leaf traits between two subspecies of *D.viscosa (D. viscosa ssp. angustissima and D. viscosa ssp. spatulata)* for similarities or differences.

This study seeks to improve the robustness of leaf wax lipids as biomarkers in palaeoclimate reconstructions by reducing uncertainty in the interpretation of such proxies.

CLIMATE AND ECOLOGICAL SETTING

The study spans the Adelaide Geosyncline ranging from the MacDonnell Ranges in central Australia to Kangaroo Island in South Australia (Fig 1). Climate ranges from hot and arid in the north to more cool and wet conditions in the south. There is also a

significant climate gradient from the Fleurieu Peninsula heading inland to the east. Mean annual temperature (MAT) of sample sites ranges between 13.9–22.7 °C and mean annual precipitation (MAP) ranges between 164–808 mm (Williams et al. 2012). *D.viscosa* is a woody shrub that is widespread in Australia and is currently found on six continents where it inhabits a large range of climatic and ecological environments (Harrington and Gadek 2009). As such, *D.viscosa* is an ideal candidate to study a single species' chemophysiological responses to environmental gradients. *D.viscosa* evolved from its most recent ancestor in Australia during the late Pliocene (Harrington and Gadek 2009). In Australia *D.viscosa* occurs in arid and semi-arid woodlands. Two subspecies of *Dodonaea viscosa, angustissima* and *spatulata*, occur along the climate gradient in this study. These two subspecies were separated on the basis of differences in SLA (West 1980). *D.viscosa* is an evergreen angiosperm with small, linear leaves and a thick waxy cuticle (Hill et al. 2015). Leaf morphology of *D.viscosa* has been documented to vary with variation in climate and it was suggested that leaf width was associated with maximum regional temperature and leaf area with minimum local temperature (Guerin et al. 2012).

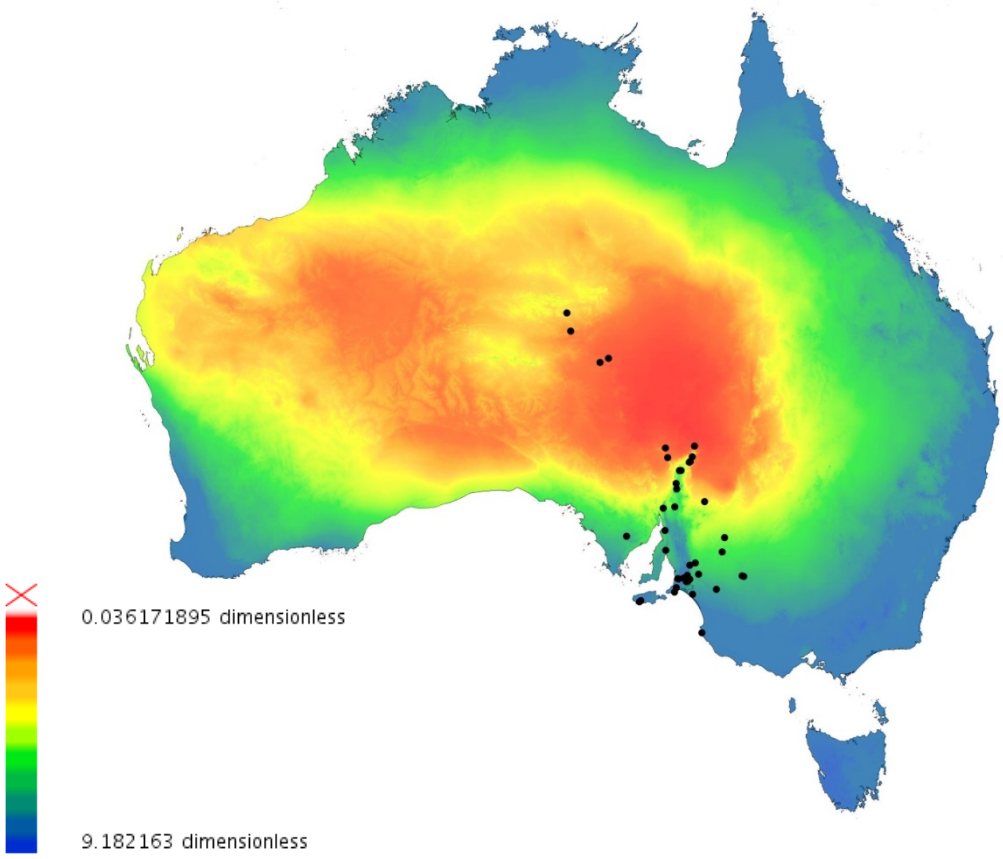

Figure 1. Map of Australia showing location of sample sites and annual mean aridity index variation. Warm colours indicate more arid areas and cool colours less arid areas.

METHODS

Sample selection

A total of 43 leaf samples were used for this study and were supplied by the Terrestrial Ecosystem Research Network and from collections assembled by Matt Christmas, Greg Guerin, Jacob Mills and Mark Laws. These samples were collected from between the MacDonnell Ranges in central Australia and Kangaroo Island off of the south coast of South Australia (for sample location coordinates, see Table 2).

To best explore the variation in *n*-alkanes with climate, locations that gave the largest range of rainfall and temperature measurements were chosen. Additionally we aimed to

ensure that trends in climate variables did not strongly co-vary with distance between samples. This was to reduce the chance of differences in leaf wax composition simply being a result of the genetic isolation by distance between individual plants. To determine whether variation in climate parameters between samples co-varied strongly with geographic distance between samples R was used to perform Mantel tests. The Mantel test correlates matrices of pairwise distances.

Climate data

Climate data for sample locations were provided by CSIRO Ecosystem Sciences and extracted from the Atlas of Living Australia website (Williams et al. 2012) (metadata for climate variables can be found in Appendix B). Description of climate variables used are given in Table 1.

Table 1. Description of climate variables.

Climate Variable	Description
MAP	Mean annual precipitation (mm/year)
MAT	Mean annual temperature (°C)
AI	Mean annual aridity index. The monthly ratio of precipitation to potential evaporation (pan, free-water surface). A numerical indicator of the degree of dryness of the climate at a given location (dimensionless values from 0.0-10).
SR	Highest period solar radiation (MJ/m2/day)

Leaf preparation

Leaf tissue samples were dried in synthetic gauze bags on silica gel and ground to a powder using a ball mill (Retsch MM400 with a Qiagen TissueLyser 24 adapter set).

Lipid extraction

Lipids were extracted from ground leaf material using a 9:1 DCM:MeOH solvent mixture. Approximately 0.1 g of finely ground leaf material was weighed into clean test tubes for each sample. Samples were covered with 5-7 mL of solvent and sonicated in a Soniclean 250TD for 15 minutes. The total lipid extract (TLE) was then pipetted out and filtered through glass fibre filter paper into a clean test tube. This process was repeated two more times and finally the ground sample was also rinsed through the filter paper using DCM. TLEs were then dried under nitrogen gas using a FlexiVap. Following drying, TLE residue was transferred into 4 mL glass vials using optima grade DCM and a pipette, with three sequential rinse and pipette transfers to ensure complete transfer of TLE.

Short column chromatography

TLEs were separated into polar and non-polar fractions using short column chromatography. TLEs and solvents were pipetted through a silica gel glass short column, prepared as follows: a Pasteur pipette plugged with a small amount of glass wool and ashed. The pipette was filled with a slurry of activated silica gel and optima grade hexane. Silica gel was kept at 105 °C for at least 24 hours prior to use for short column chromatography to eliminate any water present. The non-polar fraction (F1) was collected with 4 mL of optima grade hexane. Following this the polar fraction (F2) was collected with 4 mL of 1:1 DCM:MeOH. Non-polar fractions of the TLEs were dried under nitrogen gas using a FlexiVap. The F1 fractions were transferred into 2 mL vials with optima grade hexane and again dried under nitrogen gas.

Identification and quantification of *n*-alkanes

An internal standard was added to the non-polar fraction of the lipid extract in preparation for quantified analysis by gas chromatography-mass spectrometry. Dried F1 fractions in 2 mL vials had 900 µL of optima grade hexane and 100 µL of 100 µg/µL binapthyl solution added for a total volume of 1000 µL. Standard used for n-alkane analysis consisted of 800 µL of optima grade hexane, 100 µL of 100 µg/µL binapthyl and 100 µL of 10ng/µL C_7-C_{40} *n*-alkane standard for a total volume of 1000 µL.

Sample analyses were conducted by gas chromatography-mass spectrometry (GC-MS) operating in fullscan mode using a Perkin Elmer Clarus 500. 1µL of extract was injected into the split/splitless injector at 300°C operating in split mode with a split ratio of 20:1. A BPX5-MS capillary column of 30m length, 0.25mm ID and 0.25µdf coating was used for the separations with helium carrier gas at a 1ml/min constant flow. GC-MS analysis was, employing a temperature program of 50º held for 1 min then ramped to 310ºC at 8ºC/min and held isothermal for 12mins. Full scan data were acquired over range of 45-450 amu at approximately 3 scans per sec. Peak areas of *n*-alkanes and the internal standard were used to determine absolute concentrations of sample *n*-alkanes (for detail on *n*-alkane quantification see Appendix A).

Isotopic analysis

Ground leaf material was weighed into tin capsules. The target weight of ground leaf was 2.0 mg. Eight samples were weighed out a second time as replicates. Pure glycine, glutamic acid and triphenylamine (all calibrated to international C & N standards) were

used as standards. Weights were recorded in mg to 5 figures on a Satorius R200D balance. Samples were combusted at 1000°C in an Elemental Analyser (EuroVector EuroEA 3000) in line with a continuous flow isotope ratio mass spectrometer (Nu Instruments Nu Horizon, School of Physical Sciences, University of Adelaide). Two-point drift and size corrections based on glycine and glutamic acid were undertaken.

Specific Leaf Area (SLA)

Specific leaf area (SLA) is calculated as leaf area/dry leaf mass (cm^2/g). Leaf area was measured by scanning leaves with a scale included and measuring the leaf area with image analysis software Image J. Leaf mass was measured by weighing the dry leaf. Weights were recorded in grams to 5 figures on a Satorius R200D balance. SLA for an individual plant is the average of SLA measurements from five leaves. The majority of specific leaf area data used in this analysis was provided by Assoc. Prof. Zdravko Baruch.

Scanning Electron Microscopy

Morphological features of leaf waxes of 9 leaves were examined using scanning electron microscopy (SEM). Leaves were chosen to examine samples with a range of ACL values and samples that were from sites with a range of annual mean aridity index values. Leaves were mounted on a stage and coated with platinum in preparation for SEM. Several images were taken of each leaf. Images were produced by secondary electron imaging with a Philips XL30 using an acceleration of 10.0 kV and spot size of 3.0. Differences in leaf wax morphology were qualitatively assessed.

Data analysis

Statistical analyses were performed using R. Mantel tests were used to assess the strength of relationships between climate variables and geographic distance. Autocorrelation was performed to determine if climate variables co-varied with each other. Relationships amongst leaf traits and between leaf traits and climate variables were assessed by least-squares linear regression. Subspecies effects on relationships amongst leaf traits and between leaf traits and climate variables were also assessed by least squares linear regression.

Table 2. Sample coordinates, subspecies information, climate data and leaf measurement results. Listed in order of latitude and includes minimum, maximum and average values as well as standard errors.

Sample name	Latitude	Longitude	subspecies	MAP (mm/yr)	MAT (°C)	AI	SR ($MJ/m^2/day$)	conc. *n*-alkane ($\mu g\ g^{-1}$ dry leaf)	ACL	dispersion (d)	Norm31	$\delta^{13}C$ (‰ VPDB)	SLA (cm^2/g)
MCS DJ679	-37.18	139.77	spatulata	644	14.4	0.89	27	327.44	29.45	1.24	0.23	-28.17	81.94
MCDJ646	-35.98	136.86	angustissima	284	15.5	0.69	27.5	176.31	29.65	1.48	0.39	-27.90	45.88
MCS DJ729	-35.94	136.93	angustissima	624	15.3	0.71	27.4	243.20	30.27	1.50	0.59	-26.15	55.15
MCS DJ672	-35.70	139.34	spatulata	647	15.5	0.49	27.9	105.50	30.20	2.09	0.46	-27.32	70.00
MCS DJ586	-35.61	138.50	spatulata	439	15.2	0.68	27.4	116.82	29.97	2.26	0.32	-28.61	73.69
MCS_NG002	-35.50	140.44	spatulata	628	15.7	0.40	27.7	296.60	30.11	1.58	0.52	-26.02	40.70
MCS DJ590	-35.44	138.58	spatulata	390	14.7	0.83	27.3	740.44	29.80	1.31	0.40	-27.01	64.42
MCS DJ548	-35.21	139.04	angustissima	724	15.9	0.38	27.9	503.78	29.95	1.28	0.47	-27.84	66.60
MCS DJ735	-35.17	139.13	spatulata	393	15.6	0.41	27.9	279.08	29.70	1.57	0.29	-27.50	70.36
MCS DJ544	-35.11	139.21	angustissima	402	15.8	0.36	28	66.27	29.87	3.12	0.38	-28.22	76.53
MCS DJ483	-35.10	138.69	spatulata	370	14.8	1.01	27.3	23.70	29.92	3.38	0.11	-28.34	76.02
JMMB0901	-35.09	138.65	angustissima	808	15.1	0.87	27.3	182.18	30.13	1.54	0.53	-27.08	91.06
MCS DJ568	-35.07	138.92	spatulata	790	13.9	1.10	27.4	192.70	29.76	2.06	0.36	-28.18	60.60
VCAMDD03	-35.00	141.73	angustissima	785	16.7	0.29	28.1	34.56	29.97	1.00	0.48	-26.29	49.77
VCAMDD02	-34.98	141.65	angustissima	303	16.7	0.29	28.1	77.22	30.20	1.46	0.60	-24.11	47.98
MCS DJ537	-34.96	139.10	angustissima	299	15.0	0.58	27.9	89.36	29.63	1.87	0.23	-28.21	80.56
MCS DJ732	-34.92	139.62	spatulata	483	16.1	0.29	28	161.33	30.22	1.00	0.50	-24.84	63.02
MCS DJ726	-34.56	139.21	spatulata	314	15.1	0.47	28	284.33	29.74	1.40	0.34	-27.02	51.78
JMMOOR05	-34.48	139.47	angustissima	427	16.4	0.24	28.1	74.40	30.16	1.81	0.38	-26.63	62.52
SASMDD014	-34.04	140.71	angustissima	279	17.5	0.19	28.5	401.61	29.57	1.13	0.27	-24.59	51.38
MCS DJ697	-33.98	138.09	angustissima	247	16.3	0.37	28.5	195.91	30.33	1.16	0.63	-27.12	45.97
MCS DJ694	-33.48	140.83	angustissima	396	17.6	0.17	28.2	69.73	30.41	1.98	0.57	-25.98	53.29
MCS DJ713	-33.43	136.26	angustissima	250	16.5	0.33	28.6	122.17	30.22	2.87	0.43	-28.43	46.76
MCS DJ700	-33.20	138.05	angustissima	367	18.2	0.26	28.5	685.55	29.96	1.33	0.47	-26.75	44.98

SATFLB0009	-32.31	137.97	angustissima	351	14.8	0.42	28.7	57.79	29.70	0.91	0.35	-28.30	68.45
MCS DJ706	-32.25	138.51	angustissima	512	16.6	0.19	28.9	39.50	30.48	2.73	0.60	-26.82	66.51
MCS DJ705	-32.04	139.90	angustissima	287	16.9	0.12	29.1	40.90	30.42	1.68	0.49	-27.95	47.72
MCS DJ507	-31.53	138.60	angustissima	239	15.9	0.24	28.7	22.42	30.94	7.45	0.34	-30.66	60.08
GGBRA2A-6	-31.31	138.57	angustissima	381	16.0	0.24	28.8	192.55	30.42	2.28	0.63	-27.19	41.85
GG1128	-30.78	138.72	angustissima	370	17.1	0.15	28.8	78.90	30.54	2.01	0.62	-27.45	47.82
GGWAR-A-20	-30.78	138.80	angustissima	286	14.9	0.24	28.6	50.08	30.07	1.41	0.35	-26.63	35.64
SATFLB0006	-30.78	138.80	angustissima	383	14.9	0.24	28.6	372.58	29.73	1.75	0.32	-27.10	51.71
GG1142	-30.45	139.18	angustissima	383	17.7	0.10	28.8	39.67	30.19	1.61	0.47	-28.51	49.00
SATFLB0021	-30.41	139.22	angustissima	250	16.8	0.12	28.7	37.50	30.65	3.79	0.43	-25.03	47.38
SATFLB0022	-30.41	139.23	angustissima	278	16.5	0.14	28.7	185.73	30.31	1.81	0.55	-25.88	42.54
MCS DJ692	-30.25	138.18	angustissima	290	20.0	0.06	29.3	1557.00	30.10	1.12	0.54	-24.90	49.13
SATFLB0018	-30.22	139.32	angustissima	173	16.7	0.12	28.7	367.83	30.41	1.13	0.67	-27.26	36.75
MCS DJ728	-29.86	138.07	angustissima	283	20.5	0.06	29.6	1158.00	30.17	1.23	0.57	-24.27	49.62
MCGR9A	-29.78	139.43	angustissima	164	20.2	0.05	29.5	165.10	30.02	1.69	0.44	-25.19	52.81
SATSTP0002	-26.27	135.02	angustissima	176	22.2	0.06	29.7	602.47	30.31	1.32	0.61	-25.80	51.66
SATSTP0005	-26.10	135.42	angustissima	217	22.7	0.05	29.7	787.60	29.96	1.97	0.45	-24.34	45.60
NTAFIN0024	-24.92	133.66	angustissima	202	21.8	0.07	29.5	109.68	29.64	0.87	0.32	-27.49	42.77
NTAFIN0003	-24.13	133.48	angustissima	230	21.3	0.09	29	368.12	30.03	1.57	0.44	-27.33	51.08
Minimum								22.42	29.45	0.87	0.11	-30.66	35.63
Maximum								15.57	30.94	7.45	0.67	-24.11	91.06
Average								271.71	30.08	1.86	0.44	-26.83	56.27
Standard error								48.20	0.05	0.17	0.02	0.22	2.02

OBSERVATIONS AND RESULTS

Mantel tests on climate variables and geographic distances

Mantel tests show that climate variables do not strongly co-vary with geographic distance along this gradient (Fig 2, Appendix C). Sample locations include sites that are both geographically near to each other with large differences in climate and geographically far away from each other but with similar climate (Fig 2).

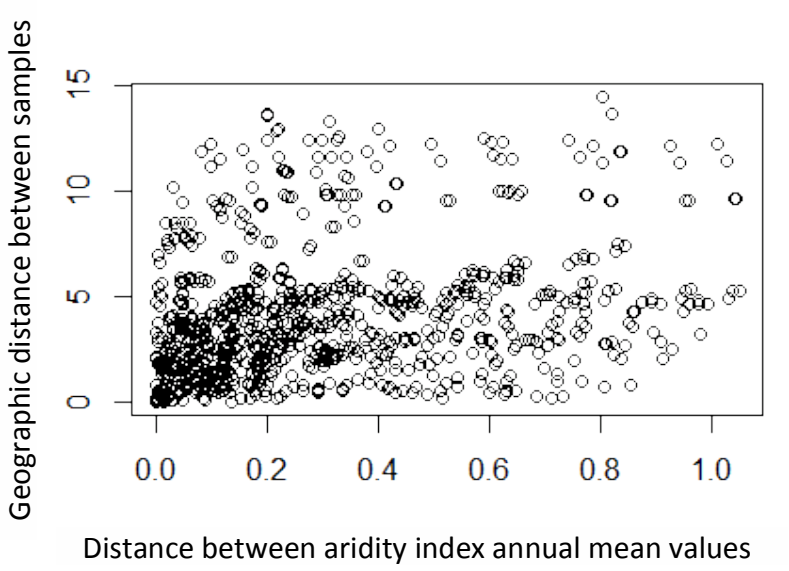

Figure 2. Output from Mantel test showing correlation between geographic distance matrix and aridity index (AI) distance matrix. Points in the top left region of the plot indicate samples that are far apart in geographic distance with similar values of AI, points in the bottom right region of the plot indicate samples that are near in geographic distance but have different values of AI.

Correlations among climate data

Auto-correlation was performed to detect correlations between climate variables. Climate variables do correlate with each other, relationships can be seen in Figure 3. Relationships between leaf traits and all climate variables were assessed using least-squares linear regression to determine which had the highest significance.

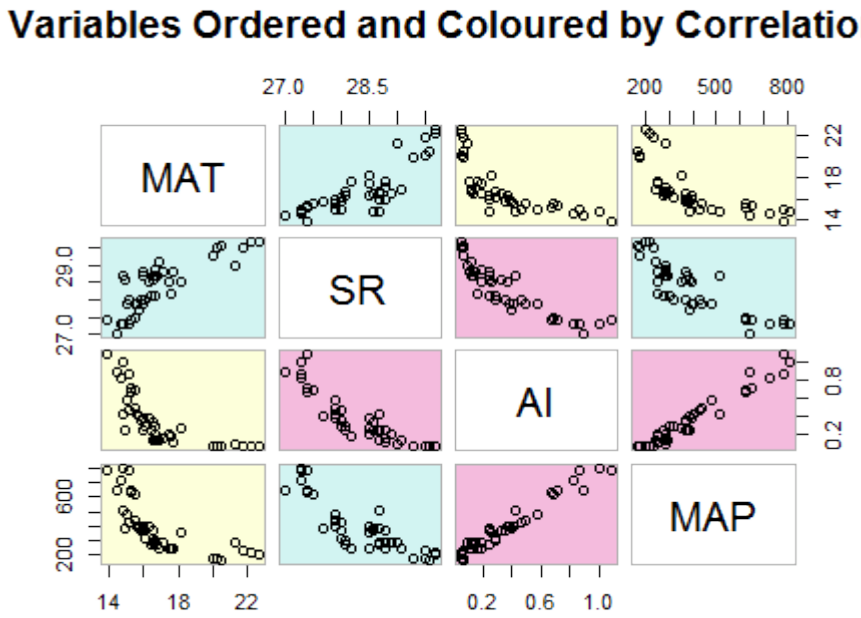

Figure 3. Correlations between climate variables. Cells are coloured by the strength of correlation between variables. Colours ordered from strongest to weakest correlation: pink, blue, yellow.

Carbon isotopes and climate

Carbon isotope ratio ($\delta^{13}C$) values ranged from -30.66 to -24.11 ‰ (mean -26.89‰, standard error (SE) 0.22 ‰) (Table 2). Least-squared linear regression results for $\delta^{13}C$ versus climate variables are given in Table 3. $\delta^{13}C$ correlates most strongly with MAP ($p=0.0013$, $R^2=0.21$), with less negative values of $\delta^{13}C$ corresponding to environments with lower MAP (Table 3). $\delta^{13}C$ also shows significant correlations with MAT ($p=0.0015$, $R^2=0.21$) and AI ($p=0.006$, $R^2=0.15$) (Fig 5a, Table 3).

SLA and climate

SLA values range from 35.64–91.06 cm^2/g (mean 56.27 cm^2/g, SE 2.08cm^2/g) (Table 2). Results from least squared linear regressions for SLA values versus climate variables are shown in Table 3. SLA shows the strongest correlation with AI ($p=8.84 \times 10^{-6}$, $R^2=0.37$). As aridity increases, SLA decreases, which translates to leaves becoming

smaller and thicker with increasing aridity (Fig 5b). SLA also shows significant correlations with MAP, MAT and SR (Table 3).

Table 3. Results of least squares linear regression between leaf traits and climate variables. R^2 and p-values are given for all comparisons, slope and intercept are given for significant relationships. Stars indicate level of significance: p-value 0-0.001= *, 0.001-0.01= **, 0.01-0.05= *.**

$\delta^{13}C$		**slope**	**intercept**	**R^2**	**p-value**
	AI	-2.08	-26.17	0.1496	0.0060**
	MAP	-0.0038	-25.41	0.2066	0.0013**
	MAT	0.30	-31.91	0.2012	0.0015**
	SR	-45.67	0.66	0.0928	0.027*
SLA		**slope**	**intercept**	**R^2**	**p-value**
	AI	29.14	45.90	0.3707	8.84×10^{-6}***
	MAP	0.044	39.10	0.3228	4.21×10^{-5}***
	MAT	-2.49	97.97	0.1568	0.0050**
	SR	10.42	351.74	0.3111	6.09×10^{-5}***
Concentration		**slope**	**intercept**	**R^2**	**p-value**
***n*-alkanes**	AI			0.01	0.24
	MAP			0.02	0.17
	MAT	66.01	-838.18	0.20	0.0018**
	SR	132.78	-3495.23	0.07	0.048*
ACL		**slope**	**intercept**	**R^2**	**p-value**
	AI	-0.48	30.24	0.16	0.0050**
	MAP	-0.00063	30.32	0.10	0.021*
	MAT			-0.01	0.41
	SR	0.15	25.88	0.09	0.027*
Norm31		**slope**	**intercept**	**R^2**	**p-value**
	AI	-0.20	0.52	0.18	0.0031**
	MAP	-0.00030	0.56	0.15	0.0059**
	MAT			0.07	0.051
	SR	0.064	-1.38	0.11	0.017*
dispersion		**slope**	**intercept**	**R^2**	**p-value**
	AI			-0.024	0.86
	MAP			-0.018	0.62
	MAT			0.0025	0.30
	SR			-0.02	0.97

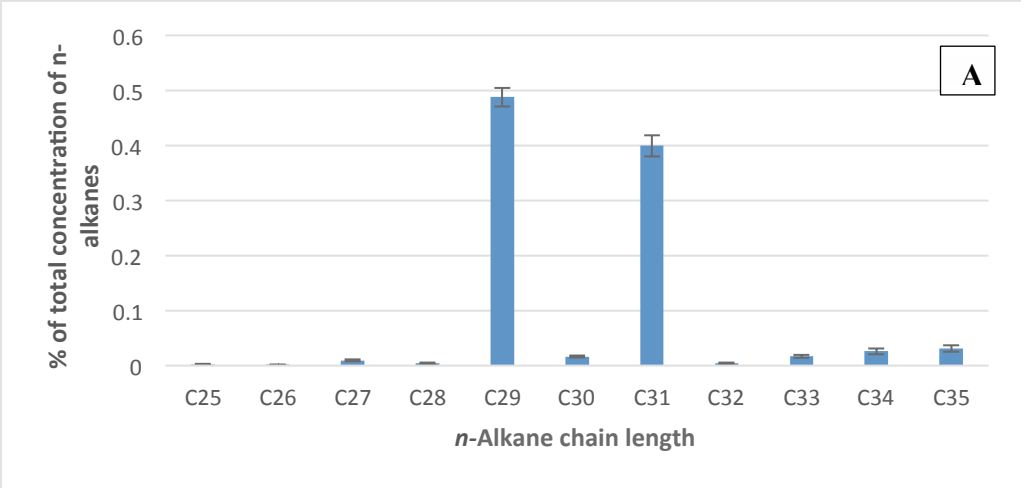

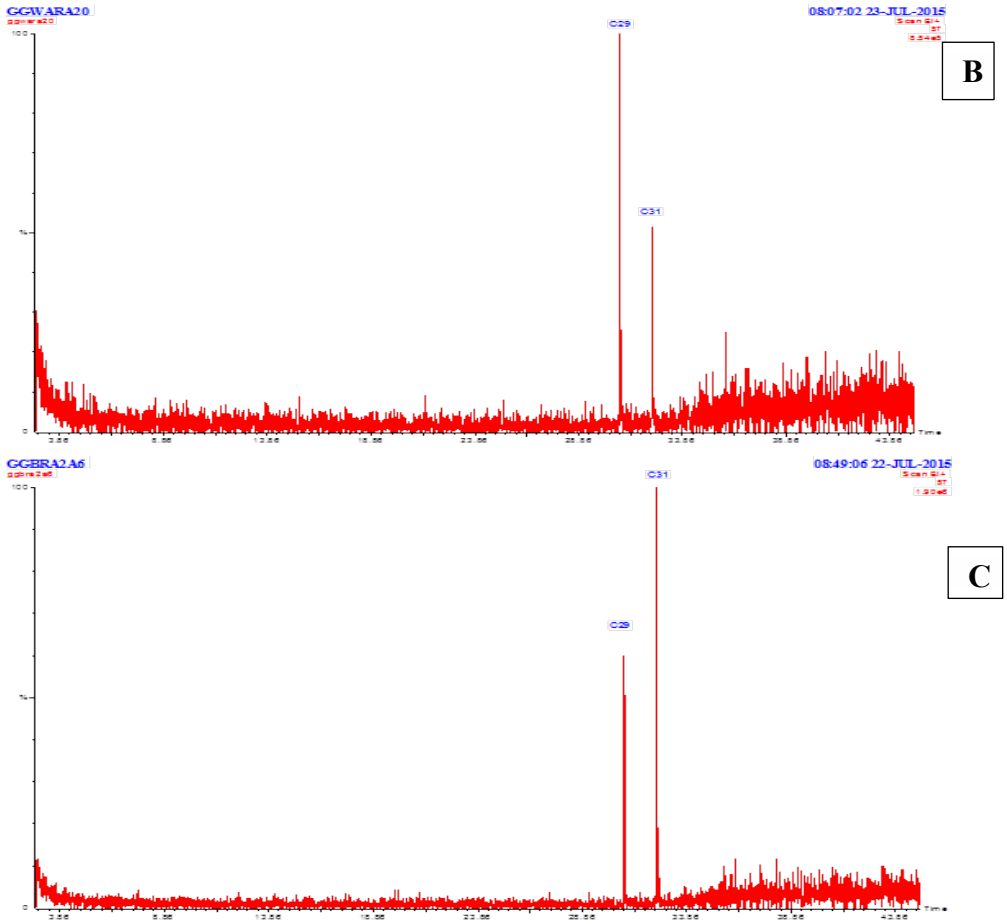

Figure 4. (A) Graph showing average values and standard error bars for the proportion of the total concentration of n-alkanes that each chain length contributes in a sample, (B) Gas chromatography-mass spectrometry (GC-MS) chromatogram of sample GGWARA20 showing C_{29} as the dominant chain length and C_{31} as the second most dominant chain length, (C) GC-MS chromatogram of sample GGBRA2A6 showing C_{31} as the dominant chain length and C_{29} as the second most dominant chain length.

n-Alkanes and climate

Leaf wax compositions of all 43 samples show two dominant chain lengths C_{29} and C_{31} (Fig 4a). *n*-Alkane profiles have a strong odd over even chain length predominance but only small amounts of other long odd numbered chain lengths (Fig 4a). The dominant *n*-alkane chain length is C_{29} in the majority of samples, with C_{31} the second most abundant chain length (Fig 4b). Samples in which C_{29} is not the most abundant chain length show C_{31} as the dominant chain length and C_{29} has the second highest abundance (Fig 4c).

CONCENTRATION

Total concentration of *n*-alkanes ranges from 22.42–1557 µg/g dry leaf (mean 271.71 µg/g dry leaf, SE 48.20 µg/g dry leaf) (Table 2). Total concentration of *n*-alkanes show a significant correlation with MAT (p= 0.0018, R^2= 0.20) and a significant correlation with SR (p= 0.048, $R^{2=}$ 0.07), but do not show significant trends with other climate variables (Table 3). Concentration of *n*-alkanes increases with increasing temperature and solar radiation (Table 3).

ACL

ACL ranges from 29.45–30.94 (mean 30.08, SE 0.05) (Table 2). Least squared linear regression results for ACL versus climate variables are presented in Table 3. ACL shows the strongest significant correlation with AI (p= 0.005, R^2= 0.16) with ACL increasing with increasing aridity (Fig 5c). ACL also shows significant relationships with MAP and SR but these are less significant than the relationship between ACL and AI (Table 3).

NORM31

Norm31 values range from 0.11–0.67 (mean 0.13, SE 0.02) (Table 2). NORM31 shows a significant correlation with AI (p= 0.0031, R^2= 0.18) (Fig 5d). Leaves grown in more arid environments have higher Norm31 values and therefore a greater proportion of C_{31} to C_{29}. Norm31 also shows significant relationships with MAP, SR and MAT though none have a greater significance than the relationship between Norm31 and AI (Table 3).

DISPERSION

Dispersion values range from 0.87–7.45 (mean 1.86, SE 0.17) (Tables 2). Due to the dominance of chain lengths C_{29} and C_{31}, dispersion is low for most samples (Fig 4a). Dispersion shows no significant relationship with climate variables (Table 3).

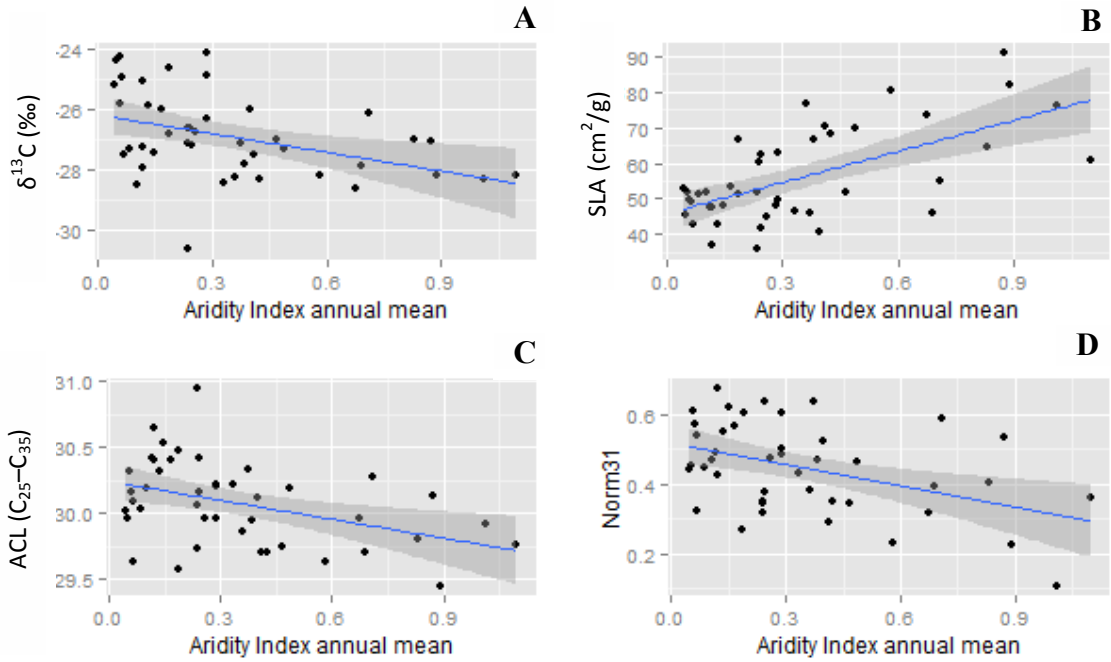

Figure 5. Aridity index annual mean vs (A) $\delta^{13}C_{leaf}$ (B) SLA (C) ACL of leaf *n*-alkanes (D) NORM31 of leaf *n*-alkanes. Regression lines are for data from 43 individuals of *Dodonaea viscosa* vs. annual mean aridity index data from the 43 sample locations. Shaded envelopes represent 95% confidence intervals. Low values of AI correspond to more arid environments.

LEAF WAX MORPHOLOGY

Scanning electron micrographs do not reveal any systematic differences in epicuticular wax morphology along the climate gradient. In the leaves examined, two types of epicuticular wax morphology are identified. These two morphologies appear to be dendritic and amorphous wax structures (Fig 6a, 6b). Surface wax appears to be degrading in several samples with the epicuticular wax layer peeling and flaking away from the cuticle surface (Fig 6c, 6d).

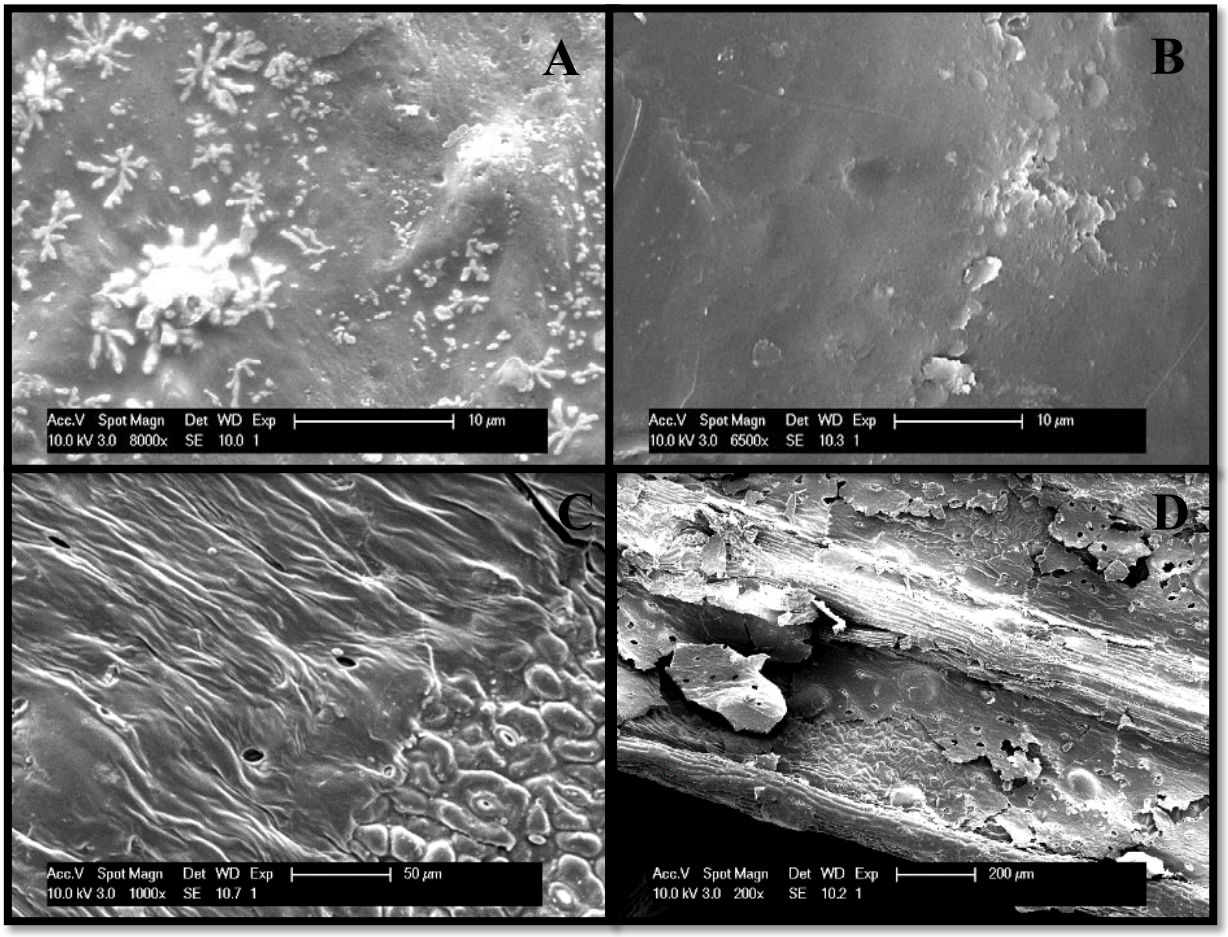

Figure 6. SEM images of epicuticular waxes on leaf surfaces: (A) dendritic wax structures on sample MCSDJ700, (B) amorphous wax on sample MCGR9A, (C) discontinuous wax layer on sample JMMB0901, (D) wax layer flaking away from the cuticle on sample MCGR9A.

Relationships among leaf traits

Results of least squares linear regressions comparing leaf trait data are given in Table 4. SLA shows significant correlations with both ACL (p= 0.025, R^2= 0.08) and $\delta^{13}C$ (p= 0.013, R^2= 0.12). There is no significant correlation between $\delta^{13}C$ and ACL (p=0.76, R^2= -0.22). There is however a significant correlation between $\delta^{13}C$ and NORM31 (p= 0.0081, R^2= 0.14). No significant relationship between dispersion and either ACL or Norm31 is found in this study.

Table 4. Results of least squares linear regression between leaf trait measurements. R^2 and p-values are given for all comparisons, slope and intercept are given for significant relationships. Stars indicate level of significance: p-value 0-0.001= *, 0.001-0.01= **, 0.01-0.05= *.**

$\delta^{13}C$		**slope**	**intercept**	**R^2**	**p-value**
	SLA	-0.04	-24.62	0.12	0.013*
	concentration	-27.43	$-1.98x10^{-3}$	0.18	0.003**
	ACL			-0.02	0.755
	Norm31	4.37	-28.84	0.14	0.008**
	dispersion	-0.57	-25.84	0.17	0.003**
SLA		**slope**	**intercept**	**R^2**	**p-value**
	concentration			0.005	0.278
	ACL	-13.05	448.51	0.08	0.039*
	Norm31	-46.67	76.87	0.19	0.002**
	dispersion			0.0002	0.321
Concentration		**slope**	**intercept**	**R^2**	**p-value**
	ACL			$-5.6x10^{-6}$	0.323
	Norm31			0.011	0.230
	dispersion	-88.82	436.39	0.072	0.046*
ACL		**slope**	**intercept**	**R^2**	**p-value**
	Norm31	1.59	29.37	0.40	$3.05x10^{-6}$***
	dispersion	0.15	29.80	0.25	0.0004***
Norm31		**slope**	**intercept**	**R^2**	**p-value**
	dispersion			0.02	0.206

Sub-species comparisons

Least squares linear regressions were used to assess if subspecies has a significant impact on relationships between leaf traits and climate variables. This was done by testing whether the additive or interactive effects of subspecies on leaf trait and climate

relationships is significant (results in Appendix D). The effect of subspecies on these relationships is found to be insignificant in all cases (Appendix D). Although sample sizes are different, both subspecies show similar relationships between leaf traits and climate variables (Figure 7). Differences in relationships of leaf traits and climate between subspecies are not investigated further, and all further analysis grouped the subspecies together.

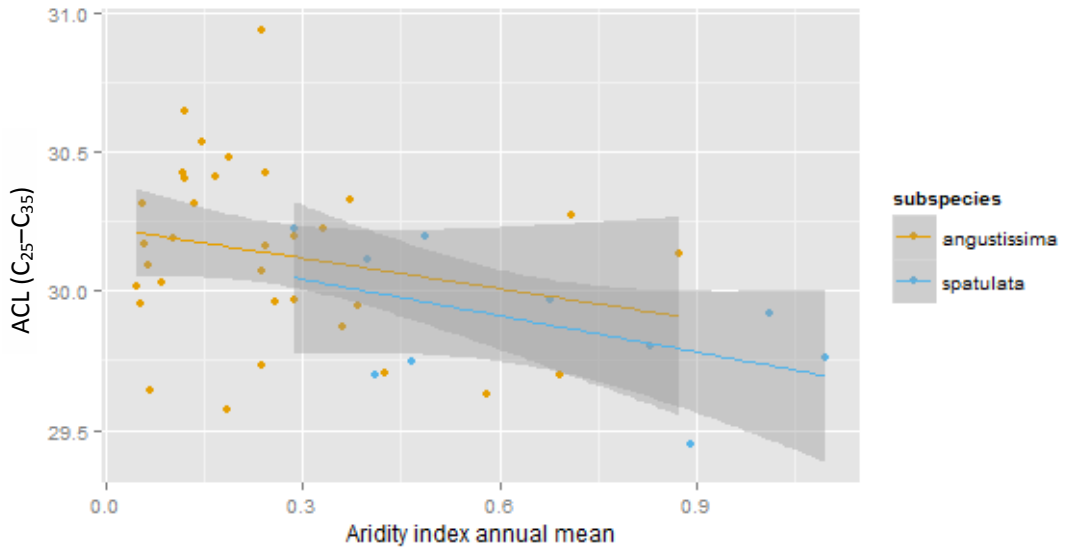

Figure 7. Aridity Index annual mean vs. ACL with data separated by subspecies. Yellow dots and regression line represent subspecies angustissima, blue dots and regression line represent subspecies spatulata. Shaded envelopes represent 95% confidence intervals. Both subspecies show similar slopes for the relationship between ACL values and annual mean aridity index.

Within Site *n*-alkane and carbon isotope data

Replication at two sites, at opposite ends of the climate gradient, was used to examine variation in *n*-alkane and carbon isotopic composition between individual plants located at the same site. *n*-Alkane ACL and carbon isotope data for five replicates at two sites are presented in Appendix E. Site A is at the cool and wet end of the climate gradient and site B is at the hot and arid end of the climate gradient. Carbon isotope ratio ($\delta^{13}C$)

values range from -28.3‰ to -25.6‰ (mean -27.44 ‰, SE 0.50 ‰) at site A and -26.38 ‰ to -24.34 ‰ (mean -25.43 ‰, SE 0.35 ‰) at site B (Appendix E). ACL values range from 29.48-29.95 (mean 29.70, SE 0.09) at site A and 29.52-30.25 (mean 29.90, SE 0.14) at site B. While within site variation is present for both *n*-alkane ACL and $\delta^{13}C$ values, the average values for each site show the same trend as the main dataset. ACL is higher and $\delta^{13}C$ values are less negative at the more arid site. Sample sizes were not large enough to statistically assess relationships between the two sites.

DISCUSSION

This study aimed to determine if within species leaf wax *n*-alkanes show variation in distribution and abundance over a climatic gradient and which climatic parameter is likely to be driving such variation. As well as examining this biochemical response to environmental stress, we also aimed to determine if *D.viscosa* displays expected physiological and anatomical responses to climate by measuring stable carbon isotope ratios ($\delta^{13}C$) and specific leaf area (SLA). *D.*viscosa was sampled from sites with a temperature range of 13.9–22.7 °C and precipitation range of 164–808 mm/yr. Predicted responses in $\delta^{13}C$ and SLA are observed in *D.viscosa*, corroborating that this species is experiencing environmental stress over this climate gradient. This provides the necessary context for interpreting *n*-alkane variation as a biochemical response to climatic stress.

Carbon isotope ratio ($\delta^{13}C$) and specific leaf area (SLA) relationships with climate

D.viscosa leaves show significantly less negative values of $\delta^{13}C$ in more arid environments (Fig 5a). This is consistent with previous work and indicates the use of water efficient strategies by individuals growing in more water limited environments (Farquhar et al. 1989, Diefendorf et al. 2010). SLA values are also consistent with previous work and expectations (Schulze et al. 2006). SLA values are significantly lower in individuals of *D.viscosa* from arid sites (Fig 5b, Table 3). Low SLA translates into leaves being smaller and thicker at arid sites, which would help prevent water loss due to leaves having a low surface area (Schulze et al. 2006). Results from this study show that individuals of *D.viscosa* are expressing these established physiological and anatomical responses to environmental stress.

n-Alkane distribution and abundance within species

Leaf wax *n*-alkane profiles of all individuals in the dataset show long chained *n*-alkanes C_{29} and C_{31} as the two most dominant chain lengths and a strong odd over even chain length predominance (Fig 4a). Both of these attributes are characteristic of *n*-alkane profiles of terrestrial plants (Eglinton and Eglinton 2008). Results from this study show that within *D.viscosa,* there is considerable variation in both the concentration of leaf wax *n*-alkanes and the dispersion (d) of *n*-alkane chain lengths around the average chain length (Table 2).

Climatic influence on *n*-alkane variation

D.viscosa n-alkane ACL and NORM31 correlate most strongly with aridity suggesting that water stress is the most likely climatic driver of *n*-alkane chain length variation in this species (Table 3). ACL and Norm31 both increase with increasing aridity (Fig 5c, 5d). This pattern was expected as the longer chain length *n*-alkanes have greater hydrophobic properties (Eglinton and Eglinton 2008, Koch and Ensikat 2008). It would therefore be beneficial for the plant to produce more long chain *n*-alkanes in arid environments to create a stronger barrier to water loss.

These finding are consistent with previous work. A study conducted in Chile on the tree species *Austrocedrus chilensis* found that more arid populations had a greater proportion of long chained *n*-alkanes than less arid populations (Dodd et al. 1998). A later study by the same authors incorporated two more species along the same transect and found that average chain length of *n*-alkanes was higher in arid site populations (Dodd and Afzal-Rafii 2000). Two studies looking at different species of the genus *Juniperus* along the Balkan Peninsula found arid populations could be distinguished from less arid populations by higher average chain length values (Rajčević et al. 2014a, Rajčević et al. 2014b). Similarly, along a transect in Australia, ACL values of the genus *Eucalyptus* increased with increasing aridity (Hoffmann et al. 2013). However, other studies in agreement with aridity being the main driver of *n*-alkane variation produced more complex results. In two African regions investigated, the more arid region showed higher ACL values than the less arid region but this could not be disentangled from the differences in species present at the two sites (Carr et al. 2014). Such complications in the interpretation of results in this study have been avoided by examining *n*- alkane

variation within a single species. Finally, Dodd and Poveda (2003) looked at *n*-alkanes along an altitudinal gradient and found higher ACL values at the lowest and highest altitudes. These findings were attributed to water stress as plants at the lowest elevation experienced summer drought and plants at the highest elevations experienced physiological drought caused by freezing (Dodd and Poveda 2003). Although MAT was identified in previous work as having a significant relationship with the ACL of *n*-alkanes, this relationship was not found in this study (Table 3) (Diefendorf et al. 2011, Pu et al. 2011, Tipple and Pagani 2013, Bush and McInerney 2015).

The dispersion of *n*-alkane chain lengths around the average chain length does not show significant correlations with climate variables as seen in some previous studies (Dodd and Afzal-Rafii 2000, Carr et al. 2014). Dispersion is low in the majority of samples due to the strong dominance of C_{29} and C_{31} chain lengths. Low dispersion has been suggested to reduce permeability of the cuticular wax layer, making it a stronger barrier to water loss (Riederer and Schneider 1990, Dodd and Afzal-Rafii 2000). It is possible that the dispersion of leaf wax *n*-alkanes is already optimised in this species

n-Alkane concentration has a significant correlation with MAT in *D.viscosa* (Table 3). Concentration of *n*-alkanes increases with increasing temperature (Table 3). Hoffmann et al. (2013) also found that concentration of *n*-alkanes in *Eucalyptus* and *Acacia* increased towards the arid end of their transect. However, in general, the effects of temperature stress on concentration of plant waxes is not clean cut with studies producing inconsistent results (Baker 1974, Shepherd et al. 1995).

Previous studies found differences in wax morphology with variation in relative humidity (Koch et al. 2006). No systematic differences in wax morphology with variation in climate are found in this study. However, this does not necessarily mean that such differences do not occur in this species. Although some dendritic wax structures are found, the majority of the epicuticular wax observed has an amorphous structure (Fig 5a and 5b). Degradation of waxes can lead to fusion of original wax structures into plate like sheets resulting in amorphous wax structure (Jeffree 2007). It is possible that leaf wax structure may have been too degraded to see differences in the specimens imaged for this study.

ACL vs. Norm31

Norm31 shows similar but stronger relationships with climate variables than ACL does (Table 3). This could suggest that the proportion of the two most abundant chain lengths better indicates the response to environmental stress. This calculation was easily applied to this dataset due to all individuals in the dataset having C_{29} and C_{31} as the most dominant chain lengths. However, in palaeorecords such as sediments, many different plants can contribute *n*-alkanes and which two chain lengths are dominant may be highly variable between different sites. If one site, for example, had C_{31} and C_{33} dominant *n*-alkanes and a more arid site had C_{33} and C_{35} dominant *n*-alkanes, the parameter Norm31 may be misleading as it would give a higher value to the less arid site. The relationship between Norm31 and $\delta^{13}C$ is significant in this study, while the relationship between ACL and $\delta^{13}C$ is not (Table 4).

Subspecies effects on leaf trait and climate relationships

To look for confounding variation introduced into the dataset by the presence of two subspecies, a combination of linear models were used to assess whether there are any significant additive or interactive effects of subspecies on the relationships of leaf traits with climate variables. No significant effects are found, allowing for the hypotheses to be examined confidently at a species level (Fig 7, Appendix E). Interestingly, relationships of SLA with climate variables and other leaf traits show no significant impact from subspecies differences. This is intriguing, as differences in SLA are the sole basis on which these two subspecies were differentiated (West 1980, West and Noble 1984).

Implications for palaeoecology

The large goal of this study was to determine if leaf wax *n*-alkanes are a tool that we could apply to the geologic past and retrieve information about climate conditions. *n*-Alkanes are highly conserved molecules which make them appealing as a potential proxy (Eglinton and Eglinton 2008). This study indicates that ACL or Norm31 in palaeo archives could provide information about changes in aridity over time. The significant relationship between Norm31 and $\delta^{13}C$ means that both these parameters could be measured on the same fossil leaf or in sediments to detect aridity with greater confidence than using a single proxy alone. In sediments and fossils compound specific $\delta^{13}C$ can be measured from *n*-alkanes rather than bulk leaf tissue (Krishnan et al. 2015).

Variation in ACL at the level of the individual is apparent from the results of the examination of ACL values from plants at the same site (Appendix E). In sediment

archives *n*-alkanes are sourced from many individual plants. ACL derived from sediments thus provides an average of many individual signals. This would reduce the impact of variability at the level of the individual on the overall signal. Concentration of leaf wax *n*-alkanes increases with increasing temperature in this study (Table 3). To the extent that this pattern is widespread, deposits derived from windblown *n*-alkanes transported from sites with large temperature differences may be biased by the greater concentration of *n*-alkanes that would be contributed by the high temperature site.

Significance

This study presents the first examination of *n*-alkane variation over a climatic gradient within a single species in Australia. In comparison to previous work on *n*-alkane variation, this study is unique as it examines leaf waxes from a shrub where previous studies have either focussed on trees, herbs, succulents or a combination of plant types from different sites. Additionally, carbon isotope ratios and specific leaf area were used to validate the assumption that the *D.viscosa* is experiencing stress due to climate conditions over the gradient studied. To my knowledge, this approach has not been considered in previous studies. To control for variation external to the parameters of interest, *n*-alkane variation was examined within species and possible subspecies effects on relationships of leaf traits with climate variables was examined statistically. The considerations made when designing this study allow for greater confidence when interpreting the results observed.

CONCLUSIONS

This study presents data from individuals of *D.viscosa* from 43 sites and finds annual mean aridity index to be the main driver of variation in ACL and Norm31 of leaf wax *n*-alkanes. In contrast to some previous studies, ACL and Norm31 show no significant relationship with MAT in this study. Results presented here also show that in this species Norm31 has stronger relationships with climatic variables and $\delta^{13}C$ than ACL has. However, the value of the use of the Norm31 parameter should be considered with caution in sedimentary environments. Concentration of *n*-alkanes shows a significant positive relationship with MAT which should also be considered when interpreting *n*-alkane data from sediments. Examination of both *n*-alkane dispersion and leaf wax surface morphology produced inconclusive results in this study as no significant relationships are found. $\delta^{13}C$ and SLA data confirm that *D.viscosa* experiences variation in climatic stressors over the gradient tested. This, in addition to accounting for effects of subspecies on the relationships of leaf traits with climate variables, sets this study apart from previous work. Results from this study can be interpreted with greater confidence due to the high degree of taxonomic control and characterisation of the plant responses to stress. The use of the distribution of leaf wax *n*-alkanes as a tool for detecting changes in aridity is supported by the findings of this study.

ACKNOWLEDGMENTS

I would like to thank Cesca McInerney and Martin Breed for their supervision, advice and encouragement. I would also like to thank Mark Rollog for isotopic analysis, Tony Hall for *n*-alkane analysis, Kristine Nielson and Jake Andre for lab and technical assistance, Stefan Caddy-Retalic for advice and editing, Zdravko Baruch Glasner for SLA data and methodology, Matt Christmas, Terrestrial Ecosystem Research Network, Greg Guerin, Jacob Mills and Mark Laws for providing leaf samples and Adelaide Microscopy for use of their facilities and in particular, Ben Wade for assistance with SEM imaging.

REFERENCES

BAKER E. 1974. The influence of environment on leaf wax development in Brassica oleracea var. gemmifera. *New Phytologist* **73**, 955-966.

BRADLEY R. S. 2015 Chapter 1 - Paleoclimatic Reconstruction. In BRADLEY R. S. ed. Paleoclimatology (Third Edition). pp. 1-11. San Diego: Academic Press.

BUSH R. T. & MCINERNEY F. A. 2013. Leaf wax n-alkane distributions in and across modern plants: Implications for paleoecology and chemotaxonomy. *Geochimica et Cosmochimica Acta* **117**, 161-179.

BUSH R. T. & MCINERNEY F. A. 2015. Influence of temperature and C4 abundance on n-alkane chain length distributions across the central USA. *Organic Geochemistry* **79**, 65-73.

CARR A. S., BOOM A., GRIMES H. L., CHASE B. M., MEADOWS M. E. & HARRIS A. 2014. Leaf wax n-alkane distributions in arid zone South African flora: Environmental controls, chemotaxonomy and palaeoecological implications. *Organic Geochemistry* **67**, 72-84.

DIEFENDORF A. F., FREEMAN K. H., WING S. L. & GRAHAM H. V. 2011. Production of n-alkyl lipids in living plants and implications for the geologic past. *Geochimica et Cosmochimica Acta* **75**, 7472-7485.

DIEFENDORF A. F., MUELLER K. E., WING S. L., KOCH P. L. & FREEMAN K. H. 2010. Global patterns in leaf 13C discrimination and implications for studies of past and future climate. *Proceedings of the National Academy of Sciences* **107**, 5738-5743.

DODD R. S. & AFZAL-RAFII Z. 2000. Habitat-Related Adaptive Properties of Plant Cuticular Lipids. *Evolution* **54**, 1438-1444.

DODD R. S. & POVEDA M. M. 2003. Environmental gradients and population divergence contribute to variation in cuticular wax composition in Juniperus communis. *Biochemical Systematics and Ecology* **31**, 1257-1270.

DODD R. S., RAFII Z. A. & POWER A. B. 1998. Ecotypic adaptation in Austrocedrus chilensis in cuticular hydrocarbon composition. *New Phytologist* **138**, 699-708.

EGLINTON G. & HAMILTON R. J. 1967. Leaf Epicuticular Waxes. *Science* **156**, 1322-1335.

EGLINTON T. I. & EGLINTON G. 2008. Molecular proxies for paleoclimatology. *Earth and Planetary Science Letters* **275**, 1-16.

FARQUHAR G. D., EHLERINGER J. R., AND & HUBICK K. T. 1989. Carbon Isotope Discrimination and Photosynthesis. *Annual Review of Plant Physiology and Plant Molecular Biology* **40**, 503-537.

GUERIN G. R., WEN H. & LOWE A. J. 2012 Leaf morphology shift linked to climate change.

HARRINGTON M. G. & GADEK P. A. 2009. A species well travelled – the Dodonaea viscosa (Sapindaceae) complex based on phylogenetic analyses of nuclear ribosomal ITS and ETSf sequences. *Journal of Biogeography* **36**, 2313-2323.

HILL K. E., GUERIN G. R., HILL R. S. & WATLING J. R. 2015. Temperature influences stomatal density and maximum potential water loss through stomata of

Dodonaea viscosa subsp. angustissima along a latitude gradient in southern Australia. *Australian Journal of Botany* **62**, 657-665.

HOFFMANN B., KAHMEN A., CERNUSAK L. A., ARNDT S. K. & SACHSE D. 2013. Abundance and distribution of leaf wax n-alkanes in leaves of Acacia and Eucalyptus trees along a strong humidity gradient in northern Australia. *Organic Geochemistry* **62**, 62-67.

JEFFREE C. E. 2007 The Fine Structure of the Plant Cuticle. Annual Plant Reviews Volume 23: Biology of the Plant Cuticle*.* pp. 11-125. Blackwell Publishing Ltd.

KOCH K. & ENSIKAT H.-J. 2008. The hydrophobic coatings of plant surfaces: Epicuticular wax crystals and their morphologies, crystallinity and molecular self-assembly. *Micron* **39**, 759-772.

KOCH K., HARTMANN K. D., SCHREIBER L., BARTHLOTT W. & NEINHUIS C. 2006. Influences of air humidity during the cultivation of plants on wax chemical composition, morphology and leaf surface wettability. *Environmental and Experimental Botany* **56**, 1-9.

KRISHNAN S., PAGANI M. & AGNINI C. 2015. Leaf waxes as recorders of paleoclimatic changes during the Paleocene-Eocene Thermal Maximum: Regional expressions from the Belluno Basin. *Organic Geochemistry* **80**, 8-17.

MA J.-Y., SUN W., LIU X.-N. & CHEN F.-H. 2012. Variation in the Stable Carbon and Nitrogen Isotope Composition of Plants and Soil along a Precipitation Gradient in Northern China. *PLoS ONE* **7**, p.e51894.

O'LEARY M. H. 1988. Carbon Isotopes in Photosynthesis. *BioScience* **38**, 328-336.

PRENTICE I. C., MENG T., WANG H., HARRISON S. P., NI J. & WANG G. 2011. Evidence of a universal scaling relationship for leaf CO2 drawdown along an aridity gradient. *New Phytologist* **190**, 169-180.

PU Y., ZHANG H., WANG Y., LEI G., NACE T. & ZHANG S. 2011. Climatic and environmental implications from n-alkanes in glacially eroded lake sediments in Tibetan Plateau: An example from Ximen Co. *Chinese Science Bulletin* **56**, 1503-1510.

RAJČEVIĆ N., JANAĆKOVIĆ P., DODOŠ T., TEŠEVIĆ V., BOJOVIĆ S. & MARIN P. D. 2014a. Leaf n-Alkanes as Characters Differentiating Coastal and Continental Juniperus deltoides Populations from the Balkan Peninsula. *Chemistry & biodiversity* **11**, 1042-1052.

RAJČEVIĆ N., JANAĆKOVIĆ P., DODOŠ T., TEŠEVIĆ V. & MARIN P. D. 2014b. Biogeographic Variation of Foliar n-Alkanes of Juniperus communis var. saxatilis Pallas from the Balkans. *Chemistry & biodiversity* **11**, 1923-1938.

RIEDERER M. & SCHNEIDER G. 1990. The effect of the environment on the permeability and composition of Citrus leaf cuticles. *Planta* **180**, 154-165.

SCHULZE E.-D., TURNER N. C., NICOLLE D. & SCHUMACHER J. 2006. Species differences in carbon isotope ratios, specific leaf area and nitrogen concentrations in leaves of Eucalyptus growing in a common garden compared with along an aridity gradient. *Physiologia Plantarum* **127**, 434-444.

SHEPHERD T., ROBERTSON G., GRIFFITHS D., BIRCH A. & DUNCAN G. 1995. Effects of environment on the composition of epicuticular wax from kale and swede. *Phytochemistry* **40**, 407-417.

TIPPLE B. J. & PAGANI M. 2013. Environmental control on eastern broadleaf forest species' leaf wax distributions and D/H ratios. *Geochimica et Cosmochimica Acta* **111**, 64-77.

WANG N., XU S. S., JIA X., GAO J., ZHANG W. P., QIU Y. P. & WANG G. X. 2013. Variations in foliar stable carbon isotopes among functional groups and along environmental gradients in China – a meta-analysis. *Plant Biology* **15**, 144-151.

WEST J. G. 1980. A taxonomic revision of Dodonaea Miller (Sapindaceae) in Australia/by Judith Gay West.

WEST J. G. & NOBLE I. R. 1984. Analyses of Digitised Leaf Images of the Dodonaea viscosa Complex in Australia. *Taxon* **33**, 595-613.

WHITESIDE J. H., OLSEN P. E., EGLINTON T., BROOKFIELD M. E. & SAMBROTTO R. N. 2010. Compound-specific carbon isotopes from Earth's largest flood basalt eruptions directly linked to the end-Triassic mass extinction. *Proceedings of the National Academy of Sciences* **107**, 6721-6725.

WILLIAMS K. J., BELBIN L., AUSTIN M. P., STEIN J. L. & FERRIER S. 2012. Which environmental variables should I use in my biodiversity model? *International Journal of Geographical Information Science* **26**, 2009-2047.

XIAO L., YANG H., SUN B., LI X. & GUO J. 2013. Stable isotope compositions of recent and fossil sun/shade leaves and implications for palaeoenvironmental reconstruction. *Review of Palaeobotany and Palynology* **190**, 75-84.

APPENDIX A: EXTENDED METHODS

Sample collection procedures

Mature *Dodonaea viscosa* leaves were collected and dried in tea bags over silica gel beads or dried and pressed between cardboard sheets. Samples collected by Ausplots, Matt Christmas, Greg Guerin, Mark Law and Jacob Mills.

Sample selection and climate data

Have access to *Dodonaea viscosa* samples collected from between the MacDonnell Ranges and Kangaroo Island (central and southern Australia).
Aim to select samples from 40 different locations that give the largest range of rainfall and temperature measurements. Additionally we aimed to ensure that trends in climate variables do not strongly co-vary with distance between samples.
Climate data was obtained by importing sample locations into the website Atlas of Living Australia's map function. Layers of climate data were applied to the map (mean annual temperature, annual maximum mean temperature, mean annual precipitation, summer precipitation, annual mean solar radiation, mean highest period of radiation, annual mean aridity index, monthly minimum aridity index, vapour pressure deficit). Climate data used were collected by Atlas of Living Australia were from CSIRO Ecosystem sciences. Climate data for each sample location were then exported into an Excel spreadsheet.
To determine whether variation in climate parameters between samples co-varied strongly with geographic distance between samples R was used to perform Mantel tests. The Mantel test correlates matrices of pairwise distances.

Grinding

Sample material: *Dodonaea viscosa* leaf material
Mass of leaf material needed for:
C & N stable isotope analysis – 0.002g
Lipid extraction – 0.1g
Samples of *Dodonaea viscosa* leaf material was weighed into Eppendorf tubes. Target weight for leaf material was 0.2 g to ensure enough material to measure stable C and N isotopes and to extract lipids from.
Two metal balls added to each Eppendorf tube for grinding
All Eppendorf tubes were labelled with sample identification codes.
Eppendorf tubes were loaded into the Ball mill and ground for two minutes (until leaf material formed a fine powder).
Prior to grinding a test sample was ground following the aforementioned procedure and run through a GC-MS to determine whether there was any contamination of the sample by plastic of the Eppendorf tube being mechanically broken down.

Weighing (for d13C and d15N)

Ground leaf material was weighed into tin capsules. The target weight for the ground leaf material was 2.0 mg. Actual weights along with sample identification codes were recorded on a weigh sheet. 20 percent of the number of samples were weighed out a second time as replicates and recorded in the weigh sheet. Standards used were glycine with weights ranging between 0.1-2.5 mg, terephthalic acid (TPA) with a target weight

of 0.5 mg and glutamic acid with a target weight on 1.0 mg. Actual weights of standards was recorded on the weigh sheet.

Lipid extraction
Lipids were extracted from leaf samples using a 9:1 DCM:MeOH solvent mixture. Approximately 0.1 g of ground leaf material weighed into test tubes for each sample. Samples were covered with 5-7 mL of solvent and sonicated in a Soniclean 250TD for 15 minutes. The total lipid extract (TLE) was then pipetted out and filtered through a glass fibre filter paper into a clean test tube. This process was repeated two more times and finally the ground sample was also rinsed through the filter paper using DCM. TLE's were then dried under nitrogen gas using a FlexiVap. Following drying, TLE residue was transferred into 4 mL glass vials using optima grade DCM and a pipette.

Short column chromatography
TLEs were then separated into polar and non-polar fractions.
Non-polar fraction was collected with 4 mL of optima grade hexane.
Following this the polar fraction is collected with 4 mL of 1:1 DCM:MeOH.
TLES and solvents are pipetted through a silica gel glass short column, prepared as follows:
Pasteur pipette plugged with a small amount of glass wool and ashed. Pipette is then filled with a slurry of activated silica gel and optima grade hexane. Silica gel was kept at 105 degrees Celcius for at least 24 hours prior to use for short column chromatography to eliminate any water present.
Non-polar fraction of the TLE was then dried under nitrogen gas using a FlexiVap. The non-polar fraction was then transferred into 2 mL with optima grade hexane and again dried under nitrogen gas.
An internal standard was added to the non-polar fraction of the lipid extract in preparation for quantified analysis by gas chromatography-mass spectrometry.
Dried F1 fractions of TLEs in 2 mL vials had 900 uL of optima grade hexane and 100 uL of binapthyl added for a total volume of 1000 uL. Standard used for n-alkane analysis consisted of 800 uL of optima grade hexane, 100 uL binapthyl and 100 uL of C_7-C_{40} *n*-alkane standard for a total volume of 1000 uL.

Alkane Quantification Methodology
Following method by Rosemary Bush (May 21, 2013)
Sample *n*-alkanes are quantified using a combination of a calibration standard and an internal
standard, which is added to both the calibration standard and the unknown sample. This methodology is borrowed from Aaron Diefendorf. The calibration standard is a homologous
series of *n*-alkanes (C_7-C_{40}, from Sigma Aldrich). The stock solution is made into a series of
diluted solutions of the following concentrations (in ng/μL): 100, 50, 25, 10, 5, 2.5, 1, 0.5. The
lower limit of FID detection range is between 0.5 and 0.1 ng.
Each of these standard concentrations is run with the internal standard added to the solution at a
concentration of 10ng/μL. The internal standard is 1-1' binaphthyl:

Binap is an unsaturated lipid, and so if removing the internal standard from a sample or standard
is necessary, the sample is simply run through a silver-impregnated silica gel column, which
separates unsaturated lipids from saturated (i.e. *n*-alkanes). Binap also has a peak that emerges
between *n*-C_{24} and *n*-C_{25}:

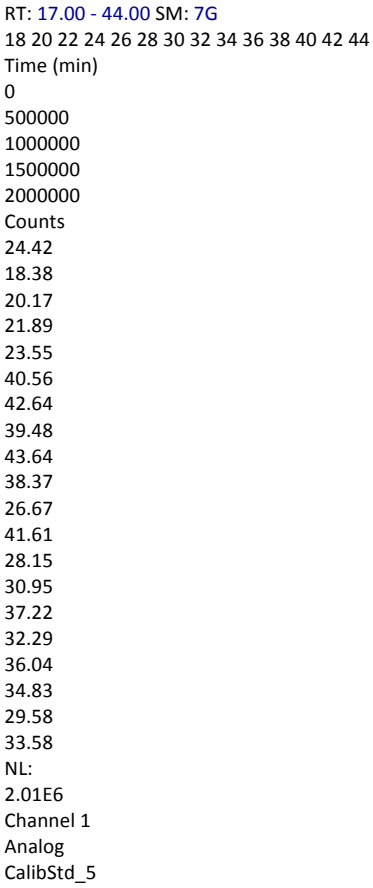

Because the internal standard is added to the calibration standards and also to the samples, the
peak areas of the sample *n*-alkanes can then be compared with the peak areas of each known
n-alkane from the calibration standard to calculate the concentration of the unknown.
An additional benefit to this method is that if the sample evaporates, or the injection syringe
draws not quite 1µL, the ratio of the internal standard is unaffected.
Calibration curves are constructed for each separate *n*-alkane. An example:
The fits for all *n*-alkanes are extremely good. Linear regression equation values for all
n-alkanes, C_{16} to C_{40}:

***n*-Alkane**	**m**	**b**	**R^2**
C16	1.520	-0.033	0.99995
C17	1.417	-0.014	0.99999
C18	1.288	-0.008	0.99998
C19	1.256	-0.007	0.99997
C20	1.227	-0.011	0.99997

C21 1.200 -0.018 0.99996
C22 1.188 -0.025 0.99995
C23 1.205 -0.033 0.99993
C24 1.225 -0.045 0.99988
C25 1.250 -0.055 0.99981
C26 1.303 -0.068 0.99970
C27 1.304 -0.078 0.99956
C28 1.362 -0.094 0.99938
C29 1.402 -0.106 0.99922
C30 1.430 -0.115 0.99912
C31 1.444 -0.120 0.99904
C32 1.487 -0.126 0.99900
C33 1.534 -0.128 0.99902
C34 1.570 -0.124 0.99911
C35 1.558 -0.118 0.99924
C36 1.582 -0.115 0.99939
C37 1.542 -0.101 0.99955
C38 1.549 -0.089 0.99970
C39 1.444 -0.071 0.99982
C40 1.461 -0.057 0.99987

Gas Chromatograpy–Mass Spectrometer for n-alkane analysis

A very powerful and sensitive instrument used to study trace amounts of chemicals in the air is a gas chromatograph connected to a mass spectrometer (GCMS). The GCMS can detect chemicals in amounts as small as a picogram. That is 0.000000000001 gram. The GCMS can separate the complex mixtures of chemicals found in air or water based on volatility. More volatile chemicals move faster than less volatile chemicals. The GCMS tells you the amount of each chemical present in a sample by comparing to a standard, a pre-measured known amount of the chemical also measured on the GCMS.

Elemental Analyser–Isotope Ration Mass Spectrometer for C and N stable isotope analysis

For determination of carbon-13 and nitrogen-15 the bulk material must first be converted to pure N2 and CO2to permit analysis by IRMS. In this technique, samples are placed in clean tin capsules and loaded into an automatic sampler. They are then dropped into a combustion furnace held at 1000 deg. C where they are combusted in the presence of an excess of oxygen. The tin capsules flash combust causing the temperature in the vicinity of the sample to rise to ca. 1700 deg. C. The gaseous products of combustion are swept in a helium stream over a Cr2O3 combustion catalyst, CuO wires to oxidize hydrocarbons and silver wool to remove sulfur and halides. The resultant gases (N2, NOx, H2O, O2, and CO2) are then swept through a reduction stage of pure copper wires held at 600 deg. C. This removes any remaining oxygen and converts NOx gases to N2. Water is removed by a magnesium perchlorate trap, while removal of CO2 is available using a selectable Carbosorb™ trap. Nitrogen and carbon dioxide are separated by a packed column gas chromatograph held at an isothermal temperature. The resultant chromatographic peaks sequentially enter the ion source of the IRMS where they are ionised and accelerated. Gas species of different mass are separated in a magnetic field and simultaneously measured by a Faraday cup universal collector array. For N2, masses 28, 29 and 30 are monitored and for CO2, masses 44, 45 and 46.

Specific Leaf Area

Specific leaf area data was obtained from Zdravko Baruch Glasner. Specific leaf area (SLA) is calculated as leaf area/dry leaf mass (m^2/kg). Leaf area was measured by scanning or taking digital photos of leaves with a scale included and measuring the leaf

area with image analysis software. Leaf mass was measured by weighing the dry leaf. SLA for an individual plant is the average of SLA measurements from five leaves.
For each individual plant scan 5 leaves with a scale included. Open scanned image in Image J.
In Image J select image and select 8 bit image.
Select image and adjust sharpness.
Select analyse and select scale. Set scale to 300 pixels =2.54 cm, aspect ratio 1.0, units = cms and select global.
Use wand tool to select leaf image, leaf image should be highlighted when selected.
Select analyse and then select measure to measure the area of the leaf.

Scanning Electron Microscopy

Morphological features of leaf waxes of 9 leaves were examined using scanning electron microscopy (SEM). Leaves were chosen to examine samples with a range of ACL values and that were from sites with a range of annual mean aridity index values. Leaves were mounted on a stage and coated with platinum in preparation for SEM. Leaves are coated in order to make the surface of the leaf conductive. Samples were loaded into the SEM six at a time. Several images were taken of each leaf. Differences in leaf wax morphology were qualitatively assessed.

APPENDIX B: METADATA FOR CLIMATE VARIABLES

Description: Temperature - annual mean (Bio01)
Short Name: bioclim_bio1
Metadata contact organization: CSIRO Ecosystem Sciences
Organisation role:
Metadata date: 2010-08
Reference date: 2008-02
Resource constraints:
Licence level: 1
Licence info:
Licence notes: Permission to re-distribute ANUCLIM outputs should be obtained from Prof. Michael Hutchinson - http://fennerschool.anu.edu.au/publications/software/
Type: Environmental (gridded) 0.01 degree (~1km)
Classification: Climate ⇒ Temperature
Units: degrees C
Data language: eng
Scope:
Notes: Data derived using ANUCLIM v6 (beta) with the new set of climate surfaces (centred on 1990), by Dr. Kristen Williams.
Keywords:
More information: http://fennerschool.anu.edu.au/publications/software/
View in spatial portal : Click to view this layer
Description: Radiation - highest period (Bio21)

Short Name: bioclim_bio21
Metadata contact organization: CSIRO Ecosystem Sciences
Organisation role:
Metadata date: 2010-08
Reference date: 2008-02
Resource constraints:
Licence level: 1
Licence info:
Licence notes: Permission to re-distribute ANUCLIM outputs should be obtained from Prof. Michael Hutchinson - http://fennerschool.anu.edu.au/publications/software/
Type: Environmental (gridded) 0.01 degree (~1km)
Classification: Climate ⇒ Solar radiation
Units: MJ/m2/day
Data language: eng
Scope:
Notes: Data derived using ANUCLIM v6 (beta) with the new set of climate surfaces (centred on 1990), by Dr. Kristen Williams.
Keywords: solar, sun
More information: http://fennerschool.anu.edu.au/publications/software/
View in spatial portal : Click to view this layer
Description: Precipitation - annual (bio12)
Short Name: bioclim_bio12
Metadata contact organization: CSIRO Ecosystem Sciences
Organisation role:
Metadata date: 2010-08
Reference date: 2008-02
Resource constraints:
Licence level: 1
Licence info:
Licence notes: Permission to re-distribute ANUCLIM outputs should be obtained from Prof. Michael Hutchinson - http://fennerschool.anu.edu.au/publications/software/
Type: Environmental (gridded) 0.01 degree (~1km)
Classification: Climate ⇒ Precipitation
Units: mm
Data language: eng
Scope:
Notes: Data derived using ANUCLIM v6 (beta) with the new set of climate surfaces (centred on 1990), by Dr. Kristen Williams.
Keywords: rain
More information: http://fennerschool.anu.edu.au/publications/software/
View in spatial portal : Click to view this layer

Description: Mean annual aridity index
Short Name: arid_mean
Metadata contact organization: CSIRO Ecosystem Sciences
Organisation role:

Metadata date: 2010-07
Reference date:
Resource constraints:
Licence level: 1
Licence info:
Licence notes: Permission required to re-distribute derivative works. Please contact Dr. Kristen Williams - kristen.williams@csiro.au
Type: Environmental (gridded) 0.01 degree (~1km)
Classification: Climate ⇒ Precipitation
Units: dimensionless
Data language: eng
Scope:
Notes: The monthly ratio of precipitation to potential evaporation (pan, free-water surface). A numerical indicator of the degree of dryness of the climate at a given location. Adapted from the index proposed by UNEP (1992; cited in Middleton and Thomas (1997)).
Keywords: evaporation, rain, precipitation, temperature
More information:
http://spatial.ala.org.au/geonetwork/srv/en/metadata.show?uuid=c592f17e-bd0f-4d9e-b76f-304f9f40d028

APPENDIX C: MANTEL TEST RESULTS

```
MAP.dists <- dist(samples$MAP)
> mantel.rtest(sample.dists, MAP.dists, nrepet = 9999)
Monte-Carlo test
Observation: 0.1953237
Call: mantel.rtest(m1 = sample.dists, m2 = MAP.dists, nrepet = 9999)
Based on 9999 replicates
Simulated p-value: 0.0357

> MAT.dists <- dist(samples$MAT)
> mantel.rtest(sample.dists, MAT.dists, nrepet = 9999)
Monte-Carlo test
Observation: 0.6989277
Call: mantel.rtest(m1 = sample.dists, m2 = MAT.dists, nrepet = 9999)
Based on 9999 replicates
Simulated p-value: 1e-04
Warning message:
In is.euclid(m2) : Zero distance(s)

> mantel.rtest(sample.dists, AIAM.dists, nrepet = 9999)
Monte-Carlo test
Observation: 0.2654792
Call: mantel.rtest(m1 = sample.dists, m2 = AIAM.dists, nrepet = 9999)
Based on 9999 replicates
Simulated p-value: 0.0087
```

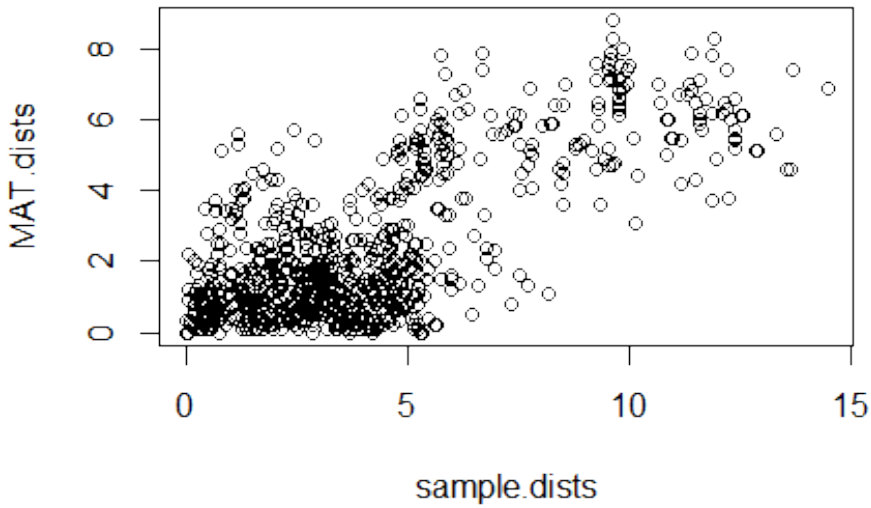

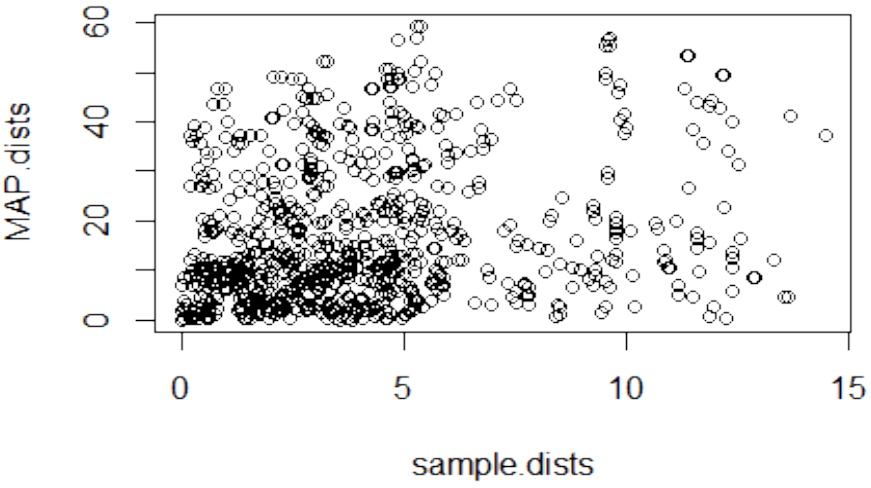

APPENDIX D: LEAST SQUARES LINEAR REGRESSIONS MODELS TESTING SUBSPECIES EFFECTS

> iAI <- lm(ACL~AI*subspecies, dodo)
> aAI <- lm(ACL~AI+subspecies, dodo)
> summary(iAI)

```
Call:
lm(formula = ACL ~ AI * subspecies, data = dodo)
Residuals:
    Min      1Q  Median      3Q     Max
-0.58616 -0.20934  0.01883  0.22083  0.79688
Coefficients:
                    Estimate Std. Error t value Pr(>|t|)
(Intercept)          30.22871    0.08355 361.787   <2e-16 ***
AI                   -0.36529    0.25548  -1.430    0.161
subspeciesspatulata  -0.05502    0.25982  -0.212    0.833
AI:subspeciesspatulata -0.07094    0.43087  -0.165    0.870
---
Signif. codes:  0 ‘***’ 0.001 ‘**’ 0.01 ‘*’ 0.05 ‘.’ 0.1 ‘ ’ 1

Residual standard error: 0.2965 on 39 degrees of freedom
Multiple R-squared:  0.1867,  Adjusted R-squared:  0.1241
F-statistic: 2.984 on 3 and 39 DF,  p-value: 0.04284
> summary(aAI)
Call:
lm(formula = ACL ~ AI + subspecies, data = dodo)
Residuals:
    Min      1Q  Median      3Q     Max
-0.58795 -0.20763  0.01849  0.22448  0.79643

Coefficients:
                    Estimate Std. Error t value Pr(>|t|)
(Intercept)          30.23512    0.07301 414.113   <2e-16 ***
AI                   -0.39023    0.20321  -1.920    0.062 .
subspeciesspatulata -0.09158    0.13316  -0.688    0.496
---
Signif. codes:  0 ‘***’ 0.001 ‘**’ 0.01 ‘*’ 0.05 ‘.’ 0.1 ‘ ’ 1
Residual standard error: 0.2929 on 40 degrees of freedom
Multiple R-squared:  0.1861,  Adjusted R-squared:  0.1454
F-statistic: 4.573 on 2 and 40 DF,  p-value: 0.01627
> id13C <- lm(d13C~AI*subspecies, dodo)
> ad13C <- lm(d13C~AI+subspecies, dodo)
> summary(id13C)
Call:
lm(formula = d13C ~ AI * subspecies, data = dodo)
Residuals:
   Min     1Q Median     3Q    Max
-3.9316 -0.8628 -0.0869  0.7116  2.7259
Coefficients:
                    Estimate Std. Error t value Pr(>|t|)
(Intercept)          -26.1875     0.3725 -70.296   <2e-16 ***
AI                    -2.2638     1.1391  -1.987   0.0539 .
subspeciesspatulata     0.8340     1.1584   0.720   0.4758
AI:subspeciesspatulata  -0.7070     1.9211  -0.368   0.7148
```

```
---
Signif. codes:  0 ‘***’ 0.001 ‘**’ 0.01 ‘*’ 0.05 ‘.’ 0.1 ‘ ’ 1
Residual standard error: 1.322 on 39 degrees of freedom
Multiple R-squared:  0.1854,  Adjusted R-squared:  0.1228
F-statistic: 2.959 on 3 and 39 DF,  p-value: 0.04404
> summary(ad13C)
Call:
lm(formula = d13C ~ AI + subspecies, data = dodo)
Residuals:
    Min      1Q  Median      3Q     Max
-3.9362 -0.8239 -0.0580  0.6822  2.7332
Coefficients:
                  Estimate Std. Error t value Pr(>|t|)
(Intercept)        -26.1236     0.3260 -80.138  < 2e-16 ***
AI                  -2.5124     0.9073  -2.769  0.00848 **
subspeciesspatulata   0.4696     0.5945   0.790  0.43432
---
Signif. codes:  0 ‘***’ 0.001 ‘**’ 0.01 ‘*’ 0.05 ‘.’ 0.1 ‘ ’ 1

Residual standard error: 1.308 on 40 degrees of freedom
Multiple R-squared:  0.1826,  Adjusted R-squared:  0.1417
F-statistic: 4.467 on 2 and 40 DF,  p-value: 0.01774

> iSLA <- lm(SLA~AI*subspecies, dodo)
> aSLA <- lm(SLA~AI+subspecies, dodo)
> summary(iSLA)
Call:
lm(formula = SLA ~ AI * subspecies, data = dodo)
Residuals:
    Min      1Q   Median      3Q     Max
-22.2788  -7.4838   0.5289   7.6005  19.6250
Coefficients:
                    Estimate Std. Error t value Pr(>|t|)
(Intercept)            44.498      2.970  14.983  < 2e-16 ***
AI                     34.263      9.081   3.773 0.000536 ***
subspeciesspatulata     8.784      9.235   0.951 0.347417
AI:subspeciesspatulata  -15.999     15.316  -1.045 0.302633
---
Signif. codes:  0 ‘***’ 0.001 ‘**’ 0.01 ‘*’ 0.05 ‘.’ 0.1 ‘ ’ 1
Residual standard error: 10.54 on 39 degrees of freedom
Multiple R-squared:  0.4026,  Adjusted R-squared:  0.3567
F-statistic: 8.762 on 3 and 39 DF,  p-value: 0.0001446
> summary(aSLA)
Call:
lm(formula = SLA ~ AI + subspecies, data = dodo)
Residuals:
    Min      1Q   Median      3Q     Max
-19.8420  -7.6740   0.1252   8.0723  20.2158
```

Coefficients:

	Estimate	Std. Error	t value	Pr(>|t|)	
(Intercept)	45.9447	2.6304	17.467	< 2e-16	***
AI	28.6383	7.3209	3.912	0.000346	***
subspeciesspatulata	0.5366	4.7974	0.112	0.911503	

Signif. codes: 0 '***' 0.001 '**' 0.01 '*' 0.05 '.' 0.1 ' ' 1
Residual standard error: 10.55 on 40 degrees of freedom
Multiple R-squared: 0.3859, Adjusted R-squared: 0.3552
F-statistic: 12.57 on 2 and 40 DF, p-value: 5.818e-05

APPENDIX E: WITHIN SITE VARIATION DATA ANALYSIS

site 1	ACLsite1	site2	ACLsite2
DJ646 1	29.65327	S05 1	29.95617
DJ646 2	29.83681	S05 2	29.52057
DJ646 3	29.4852	S05 3	30.25863
DJ646 4	29.95251	S05 4	30.06918
DJ646 5	29.56962	S05 5	29.63459
Average	29.69948	Average	29.88783
StDev	0.192222	StDev	0.305803

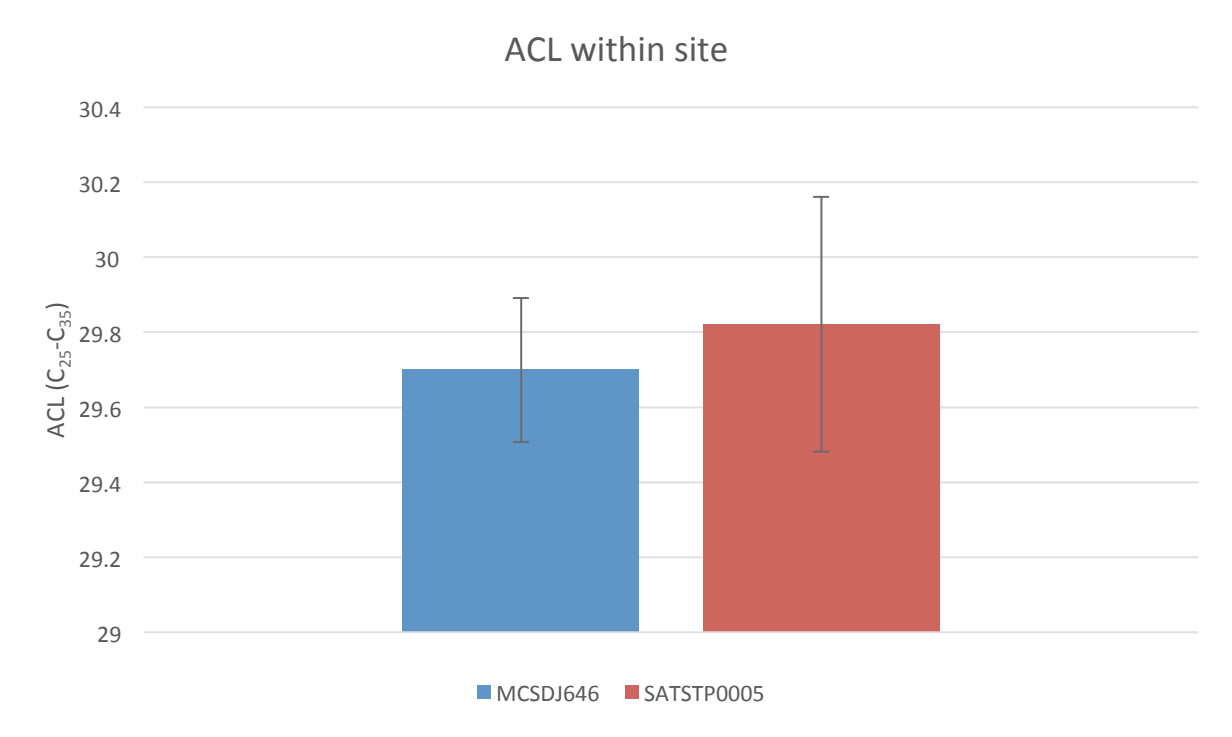

site 1	d13Csite1	site2	d13Csite2
DJ646 1	-27.9	S05 1	-24.34

DJ646 2	-27.2	S05 2	-26.3837
DJ646 3	-28.2	S05 3	-25.3467
DJ646 4	-25.6	S05 4	-25.9408
DJ646 5	-28.3	S05 5	-25.1361
Average	-27.44	Average	-25.4295
StDev	1.114899099	StDev	0.782943

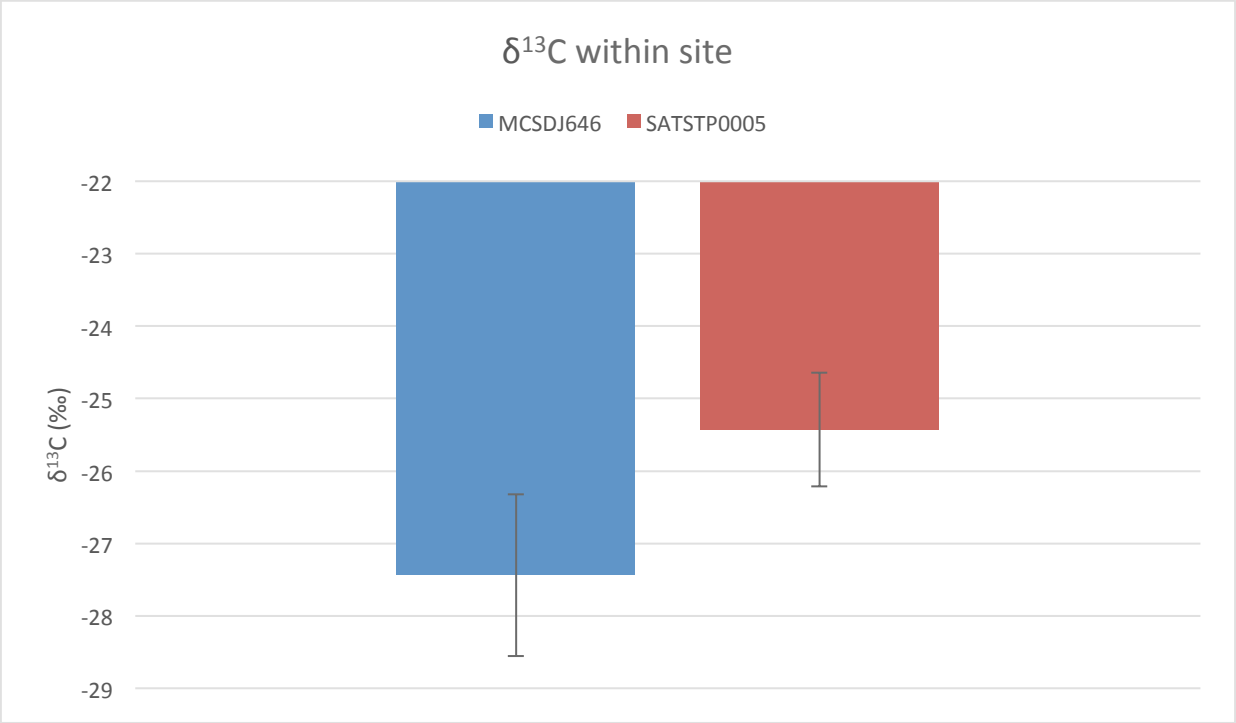

SATFLB0009	-32.31	137.97	angustissima	351	14.8	0.42	28.7	57.79	29.70	0.91	0.35	-28.30	68.45
MCS DJ706	-32.25	138.51	angustissima	512	16.6	0.19	28.9	39.50	30.48	2.73	0.60	-26.82	66.51
MCS DJ705	-32.04	139.90	angustissima	287	16.9	0.12	29.1	40.90	30.42	1.68	0.49	-27.95	47.72
MCS DJ507	-31.53	138.60	angustissima	239	15.9	0.24	28.7	22.42	30.94	7.45	0.34	-30.66	60.08
GGBRA2A-6	-31.31	138.57	angustissima	381	16.0	0.24	28.8	192.55	30.42	2.28	0.63	-27.19	41.85
GG1128	-30.78	138.72	angustissima	370	17.1	0.15	28.8	78.90	30.54	2.01	0.62	-27.45	47.82
GGWAR-A-20	-30.78	138.80	angustissima	286	14.9	0.24	28.6	50.08	30.07	1.41	0.35	-26.63	35.64
SATFLB0006	-30.78	138.80	angustissima	383	14.9	0.24	28.6	372.58	29.73	1.75	0.32	-27.10	51.71
GG1142	-30.45	139.18	angustissima	383	17.7	0.10	28.8	39.67	30.19	1.61	0.47	-28.51	49.00
SATFLB0021	-30.41	139.22	angustissima	250	16.8	0.12	28.7	37.50	30.65	3.79	0.43	-25.03	47.38
SATFLB0022	-30.41	139.23	angustissima	278	16.5	0.14	28.7	185.73	30.31	1.81	0.55	-25.88	42.54
MCS DJ692	-30.25	138.18	angustissima	290	20.0	0.06	29.3	1557.00	30.10	1.12	0.54	-24.90	49.13
SATFLB0018	-30.22	139.32	angustissima	173	16.7	0.12	28.7	367.83	30.41	1.13	0.67	-27.26	36.75
MCS DJ728	-29.86	138.07	angustissima	283	20.5	0.06	29.6	1158.00	30.17	1.23	0.57	-24.27	49.62
MCGR9A	-29.78	139.43	angustissima	164	20.2	0.05	29.5	165.10	30.02	1.69	0.44	-25.19	52.81
SATSTP0002	-26.27	135.02	angustissima	176	22.2	0.06	29.7	602.47	30.31	1.32	0.61	-25.80	51.66
SATSTP0005	-26.10	135.42	angustissima	217	22.7	0.05	29.7	787.60	29.96	1.97	0.45	-24.34	45.60
NTAFIN0024	-24.92	133.66	angustissima	202	21.8	0.07	29.5	109.68	29.64	0.87	0.32	-27.49	42.77
NTAFIN0003	-24.13	133.48	angustissima	230	21.3	0.09	29	368.12	30.03	1.57	0.44	-27.33	51.08
Minimum								22.42	29.45	0.87	0.11	-30.66	35.63
Maximum								15.57	30.94	7.45	0.67	-24.11	91.06
Average								271.71	30.08	1.86	0.44	-26.83	56.27
Standard error								48.20	0.05	0.17	0.02	0.22	2.02